First-principles modeling of spin-mixing in organic semiconductors

Dissertation
submitted for the award of the title
"Doctor of Natural Sciences"
to the Faculty of Physics, Mathematics and Computer Science
of
Johannes Gutenberg University Mainz
in Mainz

UDAY CHOPRA
Born in New Delhi, India

Berichterstatter: Prof. Dr. Jairo Sinova

Zusammenfassung

Die Forschung zu organischen Halbleitern für Spintronik-Anwendungen begann vor ungefähr zwei Jahrzehnten. In den letzten Jahren gab es mehrere Studien, welche die Spin-Relaxations- und Transportphänomene auf der Grundlage des für Festkörpermaterialien vorherrschenden Verständnisses untersuchen. Die Mischung von entgegengesetzten Spins aufgrund von Spin-Bahn Kopplung (SBK) wurde als einer der Hauptantriebsfaktoren für die Spin-Relaxation identifiziert. Der Grad der Spinvermischung in organischen Materialien kann leicht theoretisch berechnet werden und hilft bei der Vorhersage bedeutender spintronischer Phänomene. Die meisten Arbeiten in der vorhandenen Literatur verwenden jedoch grobe Analysetechniken oder semiempirische Annäherungen. Ziel dieser Arbeit ist es, einen Ansatz nach sogenannter "first-principles" Theorie einzuführen. Dieser ermöglicht ein besseres Verständnis von Spinrelaxation in organischen Materialien unter Verwendung des Spin-Mischungsparameters (γ). Wir präsentieren einen verallgemeinerten, parameterlosen Formalismus und demonstrieren seine Genauigkeit und Übertragbarkeit auf verschiedene Klassen für die Spintronik relevante organische Verbindungen, einschließlich molekularer Magnete. Dieser Ansatz ist für sogenannte "high-throughput" Rechenstudien einfach zu implementieren und die Genauigkeit seiner Vorhersagen wurde mit Experimenten verglichen. Die Ergebnisse unterstreichen auch die Komplementarität unserer Herangehensweise zu Experimenten, da γ als theoretisches Entwurfswerkzeug zur Abstimmung des SBK in Molekülen verwendet werden kann.

Abstract

Research in organic semiconductors for spintronic applications was initiated roughly two decades ago. In recent years, there have been several studies that investigate the spin-relaxation and transport phenomena based on the understandings prevalent for solid state materials. Spin-mixing in opposite spin states due to the spin-orbit coupling (SOC) has been identified as one of the major driving factors for spin-relaxation. The degree of spin-mixing in organics can be easily calculated from theoretical techniques and assist predictions of essential spintronic phenomena. However, most of the work in literature use crude analytical techniques or semi-empirical approximations. The aim of this thesis is to introduce a first-principle approach that enable a better understanding of spin-relaxation in organics using the spin-admixture parameter (γ). We present a generalized formalism, void of any parameters and demonstrate its accuracy and transferability across different classes of organic compounds relevant for spintronics, including molecular magnets. This approach is easy to implement for high-throughput computational studies and its predictive accuracy has been benchmarked against experiments. The results also emphasize the complementarity of the approach to the experiments as γ can be used a theoretical design tool to tune the SOC in molecules.

Contents

List of Figures

List of Tables

Chapter 1

Introduction

The end of the 20^{th} century was marked by an entrance to the information age which is largely governed by electronics and computer science. Evolution of micro-electronics has assisted several of the crucial scientific advancements in the last few decades, ranging from the internet to the large-scale application of machine-learning and modern-day *smart* devices. In order to tend to the rising amounts of information generated by these technologies, there is an ever increasing need to be able to store the data in more compact forms. Furthermore, a faster and more efficient processing of that information is required. However, there's a limitation on that imposed by Moore's Law[1], which states that the number of transistors on a microprocessor doubles every two years and this requires the transistors to become smaller.

An emergent technology called spintronics or spin-based electronics has been pushing Moore's law to its limits by giving rise to higher density storage materials. Combined with nano-electronics, the size of processors has also diminished. This can also be observed from trends in Intel's microprocessor architectures[2] which shows an increase in clock speeds and decrease in size of processing units, both by three orders of magnitude. More recently, spintronic devices based on organic semiconductors have also opened up a vast scope of possibilities to explore the phenomenon at a nanoscale.[3] However, the nascent field of organic spintronics has not been fully exploited as much remains to be understood about the spin-transport in such materials.

Spintronics centers on utilizing the spin-degree of freedom of the electron alongside the motion of it's charge. Electron spin has been a central concept in the foundations of quantum mechanics, and it's influence on conductivity of electrons was first suggested in 1936 by Mott.[4] The first influential spin-

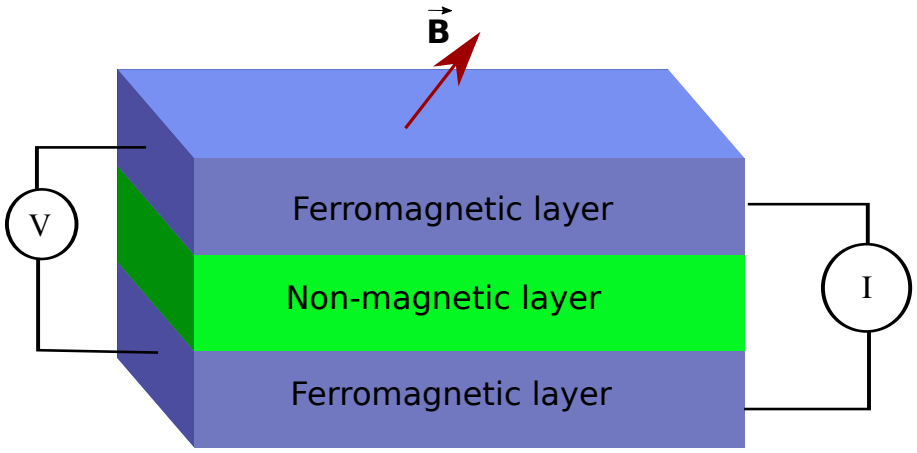

Figure 1.1: Schematic of a spin-valve device consisting of a non-magnetic (NM) layer sandwiched between two ferromagnets (FM).

tronic application came about three decades ago from the pioneering works of Grünberg[5] and Fert[6] winning them the Nobel prize in Physics in 2007. They devised a spin-valve in which they discovered the giant magnetoresistance (GMR) effect using which the device could be operated at low (off) and high (on) - resistance states only by varying the magnetic field.

The schematic of Grünberg's[5] original spin-valve device is shown in Fig. 1.1. An efficient spintronic device relies on a spacer layer that should be long enough to decouple the magnetic electrodes. In addition to that, it must (a) allow for an efficient spin-injection from the FM electrode, (b) carry the spin-currents without loss of coherence for longer distances and times. The latter requires a material with a small spin-orbit coupling (SOC), an interaction arises as a relativistic effect resulting from interaction of spin with the nuclear potential under which the electron moves.

Discovery of GMR revolutionized the IT industry, allowing for high-density magnetic storage devices and more efficient read-write heads in hard disks. Consequently, this led to discovery of more crucial technology like magnetic-tunnel junctions[7, 8] and magnetoresistive-RAMs.[9] It also opened up pathways for emerging nanotechnology for different material considerations which could further enhance spintronic properties.

Organic semiconductors (OSC) are fairly new entrants to this field and ideal candidates.[10–12] As organic materials are composed of lightweight elements, the SOC is rather small compared to inorganic counterparts. This im-

plies a slower decay of spin-polarization that make organic materials favorable for spintronic applications. Not only are organic materials abundant, hence, industrially economical, they can also be tailored using synthetic chemistry to tune their electronic properties.

OSC have also proven to be successful in several other applications such as as photovoltaics [13, 14] and field-effect transistors.[15, 16] Organic LEDs (OLEDs)[17] are a phenomenal example of the advantage of organic materials as they can be easily processed in from of thin layers leading to energy efficient devices that is beyond capacities of a traditional inorganic semiconductor. Pioneering experiments in organic spintronics have successfully employed some OSCs in spin-valves.[18, 19]. Some molecules have demonstrated exceptionally large spin-relaxation times[20] and diffusion lengths.[21]

A key to understanding spin-transport in organics materials is to understand the charge-transport which vastly differs from inorganic semiconductors. Most inorganic solids tend to form clusters of regular periodic crystals due to strong covalent bonds where the valence electrons are often weakly bound by the atomic potential as represented in Fig. 1.2. On the other hand, organic materials often lack order and occur in amorphous morphologies and in semi-crystalline nature are held together by the weak Van der Waals interactions. This leads to the electrons being localized to individual units. This implies that both the charge- and spin-transport in OSC are directly correlated to each other and spin-transport primarily takes places via the charges hopping from one site to another.

Despite of the recent developments in experiments, there still remains a vast scope to promote understanding of spin-relaxation and transport in organic materials. Moreover, first-principle electronic structure calculations have become indispensable to experiments to attain a better understanding of physical phenomena. In addition to it, properties difficult to measure experimentally can be predicted using theoretical tools with limited effort and consistent accuracy, thereby achieving a complementarity with the experiments.

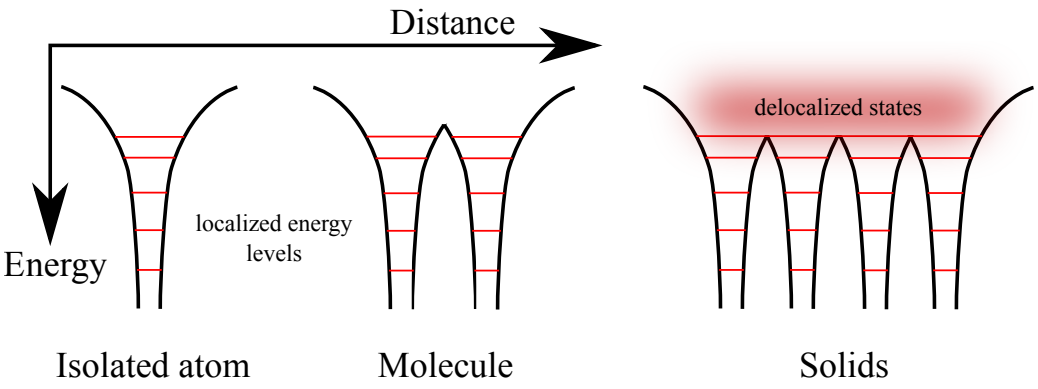

Figure 1.2: Localization vs delocalization of electronic states in molecules and solids respectively due to differences in atomic potentials

Herein lies the main objective of this thesis i.e., to investigate and model spin-relaxation in organic semiconductors using first-principle methods. The thesis is organized as follows, chapter 2 describes a brief summary of recent research in organic spintronics to explain the challenges. The first-principle methods used to tackle the problem are described in the chapter 3. Chapter 4 introduces the theoretical foundation of spin-admixture parameter inspired from the Elliot-Yafet mechanisms which has been found to be one of the dominating mechanisms in organics at normal operating conditions. Chapter 5 focuses on how chemistry can be used to tune SOC in molecules leading to design of an ideal molecule for spintronics. Finally, and outlook is presented on carrying the work forward in the direction of theoretical developments.

Chapter 2

Overview of spin-relaxation and transport in organic semiconductors

Understanding of various spin-transport and relaxation processes is crucial for designing spintronic devices with required characteristics. Such processes are intricately governed by the interactions that the itinerant spins experience within materials.

The spins can interact with intrinsic magnetic moments of the nuclei and that of neighboring electrons giving rise to the hyperfine, and spin-exchange and dipole interactions respectively. In addition to that, the spin-orbit coupling (SOC) combined with electron scattering due to impurities or lattice vibrations across different momentum states can also cause spin-relaxation.

SOC is a relativistic interaction that originates from the motion of an electron under the influence of a nuclear potential (V) which corresponds to an effective magnetic field, B_{SOC} ($\sim -\mu_B(\nabla V \times \mathbf{p})/mc^2$) w.r.t. the rest frame of the electron, where $\mathbf{p}$ is the electron momentum and μ_B is the Bohr magneton. A full relativistic treatment was first described by Dirac.[22]

The spins experience a Larmor precession under B_{SOC} with a frequency that is proportional to the momentum of that electronic state and orientation of the nuclear field. As the electrons are randomly scattered between different momentum states, the B_{SOC} also changes causing a random fluctuation of the Larmor frequencies, ω_{SOC}. These random fluctuations cause a net dephasing of the spin-polarization. This is the well known Dyakonov-Perel[23] mecha-

nism of spin-relaxation that occurs in systems lacking inversion symmetry. The spin-relaxation rate can be expressed as,

$$T_{1_{DP}}^{-1} = \omega_{SOC}^2 \tau \tag{2.1}$$

where τ is the momentum relaxation time.

Another consequence of SOC arising from the lattice is an admixture of the spin-up and down Bloch states. Momentum scattering due to lattice phonons between these admixed states causes a spin-flip. This process is called the Elliot-Yafet spin-relaxation [24, 25] and the relaxation time is described as

$$T_{1_{EY}}^{-1} \propto \omega_{SOC}^2 / \tau \tag{2.2}$$

As can be noticed, while both D-P and E-Y relaxation are proportional to the SOC, they have an inverse dependence on τ and hence the conductivity of the system. Larger conductivity implies more spin-flip scattering events and a stronger E-Y relaxation. This also means that spins precess for a shorter duration, thereby causing a weak D-Y relaxation.

The mechanisms discussed above are well-known to describe relaxation and transport phenomenon in solid-state materials. In context of organic materials, while the inherent interactions that electron spins experience in organics are similar, the transport is vastly different compared to inorganic materials. Most important distinction arises due to the charge-transport in organic materials. A review on charge-transport can be found here.[26] This consequently affects the relaxation pathways.

Spin-spin interactions such as dipolar and exchange interactions, in disordered organic semiconductors, are facilitated via a high carrier density. Exchange interactions cause two neighboring spins of opposite sign to exchange their polarity. As a consequence, the overall polarization is conserved under exchange and doesn't contribute to longitudinal spin-relaxation but to spin-transport. Exchange interactions depend on carrier density and the extent of delocalization of the spin on the molecule and when present, tends to cause a faster spin-transport.[27]

An important distinction between inorganic and organic semiconductors is that in the latter the charge-transport takes place via a spatial charge transfer between donor-acceptor states driven by intra- and inter-molecular vibrations instead of momentum scattering between electronic states. Hence, the effect of D-P and E-Y mechanisms is vastly different.

SOC in organic materials is often very small, therefore ω_{SOC} is weak. However, due to the presence of atoms with a finite nuclear spin, such as hydrogen, the local hyperfine (HF) fields can be dominant. Therefore, an analogue of D-P mechanism in organics is driven by precession under the HF fields instead of the SO fields. The role of HFI in spin-transport was observed by Nguyen *et al.*[28] where they found a suppressed relaxation on deuteration of hydrogen atoms in DOO-PPV polymers. As mentioned before, this mechanism is explicitly dependent on the charge-dynamics which is largely influenced by the energetic disorder and the temperature and therefore is likely to happen when the charge-mobility is small i.e., either at low-temperatures or in systems with large energetic disorder given that HF fields are strong. This phenomenon was explored in detail in references [27, 29].

In presence of an external field, intra-molecular vibrations combined with SOC and HFI can cause a spin-flip transition between the Zeeman states. This phenomenon, known as spin-phonon coupling, is mainly responsible for a local spin-relaxation [30–34] which can occur via direct Orbach[35] or higher order Raman-processes.[36] At extremely low temperatures, tunneling effects are also known to arise.

However, for organic semiconductors in doublet state at a reasonable magnetic fields (0.1-1 cm^{-1}), the Orbach processes are unlikely as lowest energy vibrations are at least an order of magnitude higher. Therefore, Raman processes are most likely where the spin-flip transitions are governed by a simultaneous absorption and emission of a pair of phonons.

Furthermore, in organic or molecular semiconductors characterized by inter-molecular hopping transport, spatial scattering between mixed spin states therefore works in direct analogy to, and with equal importance for spin dynamics as E-Y relaxation. Spin-mixing in these scattering states is often weak, and correspondingly well described perturbatively in SOC. The first-order perturbation correction to the spin-free Hamiltonian, a.k.a. the spin admixture parameter γ, has been derived for crystalline semi-conductors,[24, 25] molecules,[37] and more recently, for molecular electronic structure theory.[38, 39] The spin-relaxation time is proportional to the charge-hopping frequencies and spin-admixture.[39]

$$T_1^{-1} = \frac{16}{3}\gamma^2\omega \tag{2.3}$$

The active mechanism of spin-relaxation and transport depends largely on the experimental conditions and may vary extensively within the same mate-

rial. For example, if we consider the case of a molecule, Alq_3, Jiang *et al.*[40] measured spin-currents in an Alq_3 device with high-carrier concentrations ($N \sim 10^{19}$ cm^{-3}) where they attributed the transport to be dominated by exchange coupling between the spins because the spin-diffusion length was shown to be unaffected by variations in temperature. On the other hand, Drew *et al.*[41] show a clear temperature dependent MR and spin-diffusion measurements which is indicative of E-Y type spin-flips or a local thermal driven relaxation. Similarly, μSR measurements from Nuccio *et al.*[34] suggest a local spin-relaxation that is dependent on SOC at higher temperatures however independent of SOC at lower temperatures.

Harmon and coworkers [42, 43] presented a generalized model to simulate transport in amorphous systems on a regular lattice. They were able to map the effect of several of the mechanisms discussed above simultaneously, based on a characteristic waiting time-distribution. Their model is able to successfully capture the effects of different mechanisms by its sensitivity on parameters that represent the corresponding mechanisms, most significant of which are the HF fields (B_{HFI}), charge-hopping frequencies (ω), spin-mixing (γ) on-site spin-relaxation rates (Γ).

There exists several first-principle methods to calculate B_{HFI} and ω. Some recent works[44–46] also explore a detailed first-principle modeling of on-site spin-relaxation rates (Γ) driven via spin-phonon couplings. However, γ still remains unexplored except for the original works from Yu[38, 39]. Furthermore, considering high-mobility polymers as the ideal candidates for spintronic applications, it is evident from the above discussion that under reasonable operating conditions of room-temperature and low external fields, a hopping-driven spin-flip mechanism is most likely to cause the spin-relaxation.

Despite the fact that γ has become a vital parameter in a range of influential molecular spin dynamics models,[38, 39, 47] and a central concept for current experimental[48–53] and theoretical[40, 42, 43, 54–57] molecular spintronics, no further attempts to calculate or analyze γ from first-principles theory have been made, likely because of the significant methodological limitations of its current formulation.[39] In this formulation, calculations of γ are restricted to π-orbitals in organic molecules and a wave function quality below current standards of electronic structure modeling.

Therefore, accurate modeling of the spin-admixture parameter and its influence on spin-relaxation in organic compounds is the main focus of this thesis.

Chapter 3

Methods: First-principles modeling

The contents of this chapter are only intended to be a brief review of computational methodology, primarily the density functional theory (DFT) used in the thesis. For more insights into individual topics, the reader is referred to the standard textbooks of Jensen[58] and, Szabo and Ostlund[59] or review by Jones[60]

3.1 Many-body problem

The goal for most of the problems in first-principles modeling entails on calculating the ground-state electronic structure of the system. This involves solving the Schrödinger's equation,

$$\mathbf{H}\Psi = E\Psi \tag{3.1}$$

where the time-independent Hamiltonian operator contains the kinetic and potential energy terms,

$$\hat{H} = \hat{T} + \hat{V} = -\sum_{i}^{N} \frac{\hbar^2}{2m_i} \vec{\nabla}_i^{\,2} + V(\mathbf{r_1}, \mathbf{r_2}, ...\mathbf{r_N}) \tag{3.2}$$

Given that our interest lies in calculating properties of molecular systems, we further decompose the Hamiltonian in nuclear and electronic coordinates. Since the nuclei (e.g., of Hydrogen atom) is roughly 1800 times heavier

than electrons, they behave stationary w.r.t the latter due to their much smaller momentum. Therefore, the electronic and nuclear degrees of freedom can be considered independent of each other. This is termed as the Born-Oppenheimer (BO) approximation.[61] Writing the Hamiltonian in the atomic units we get,

$$\hat{H} = -\frac{1}{2}\sum_{i=1}^{N}\nabla_i^2 - \sum_{i=1}^{N}\sum_{k=1}^{M}\frac{Z_k}{\mathbf{r}_i - \mathbf{r}_k} + \sum_{i=1}^{N}\sum_{j>1}^{N}\frac{1}{|\mathbf{r}_i - \mathbf{r}_j|} + E_{\text{nuc}} \tag{3.3}$$

where the first two terms in the above equation are the one-electron term, third term represents the Coulomb repulsion between the electrons and last term is the nuclear kinetic energy. While the BO approximation simplifies the problem, exactly solving it is computationally feasible only for single-electron systems, such as the Hydrogen atom, as the position variables in second term in Eq. 3.3 cannot be separated. For complicated systems, variation principle is used as a basis for further approximations. It requires (a) assuming a suitable choice for the wave function of the system dependent on certain parameters (b) minimizing the energy expectation value by varying the parameters of the wave-function. More accurate the wave-function, closer is the solution to the true-ground state of the system.

Various approximations that were significant to the development of quantum-chemical approaches are discussed as follows.

3.1.1 Hartree Approximation

D. R. Hartree[62] assumed that the electrons exists as point charges and the only interaction that exists is the Coulomb repulsion of those point charges with a cloud of uniform electron density. This represents a simplified mean-field approximation where the electronic wave function can be expressed as a product of independent orbitals corresponding to each electron.

$$\Psi(\vec{\mathbf{r_1}}, \vec{\mathbf{r}_2}, ...\vec{\mathbf{r}_N}) \approx \phi(\vec{\mathbf{r}_1})\phi(\vec{\mathbf{r}_2})...\phi(\vec{\mathbf{r}_N}) \tag{3.4}$$

Subjected to constraints under the variational principle that the set of individual orbitals $\{\phi(\vec{r_i})\}$ are orthonormal, the ground-state energy, also called the total ground-state Hartree Energy (E_{HA}), can be calculated as follows,

$$E_{\mathrm{HA}} = -\frac{1}{2}\sum_{i=1}^{N}\int d^3\mathbf{r}\phi_i^*(\mathbf{r})\nabla_i^2\phi_i(\mathbf{r}) - \sum_{k=1}^{M} Z_k \int d^3\mathbf{r}\phi_i^*(\mathbf{r})\left|\mathbf{r}-\mathbf{r}_k\right|^{-1}\phi_i(\mathbf{r}) + \frac{1}{2}\sum_{i,j=1}^{N}\int d^3\mathbf{r}d^3\mathbf{r}'\phi_i^*(\mathbf{r})\phi_j^*\left(\mathbf{r}'\right)\left|\mathbf{r}-\mathbf{r}'\right|^{-1}\phi_j\left(\mathbf{r}'\right)\phi_i(\mathbf{r}) = T_0 + E_{\mathrm{ext}} + E_{\mathrm{H}} = \sum_{i=1}^{N}\epsilon_i \tag{3.5}$$

As can be seen from the above equation, the total energy can be expressed a sum of single particle energies containing three components, kinetic energies, nuclear-electron Coulomb energy (external) and the Hartree potential energy, respectively. The last term in 3.5 essentially corresponds to potential due to other electrons in which the electron i moves. Excluding the electron under consideration from summation in Hartree energy physically corresponds to adding a screening effect due to other electrons.

The Hartree equations are easily transferable and form a self-consistent field approach and the scaling of Hartree solutions is N^3, there exists following two major problems with the solutions:

1. The solution contains a self-interaction error, which corresponds to the electron interacting with it's own charge-density. While this can be partially corrected by restricting the summation over only other electrons, it essentially corresponds to including strong screening effects by excluding one electron from the system and often leads to inaccurate solutions.

2. Electrons being Fermionic in nature are expected to have an anti-symmetric wave-function, which is completely neglected under the Hartree approximation.

Fock suggested a possible solution to the second problem stated above.

3.1.2 Hartree-Fock Theory

Building up on the mean-field approximation by Hartree, Fock used a Slater determinant to satisfy the anti-symmetry conditions on the wave-function.

$$\Psi = \frac{1}{\sqrt{N!}}\begin{vmatrix} \phi_1\left(\mathbf{r}_1\right) & \cdots & \phi_N\left(\mathbf{r}_1\right) \\ \vdots & \ddots & \vdots \\ \phi_1\left(\mathbf{r}_N\right) & \cdots & \phi_N\left(\mathbf{r}_N\right) \end{vmatrix} \tag{3.6}$$

Using the above wave-function to evaluate the single- and many-electron terms in the BO Hamiltonian in the Eq. 3.3 led to the following Hartree-Fock equation.

$$\hat{F}\phi_k = \epsilon_k \phi_k \tag{3.7}$$

where the Fock operator is defined as

$$\hat{F} = \hat{h_1} + \sum_{i}^{N} (\hat{J}_i - \hat{K}_i) \tag{3.8}$$

The one-electron operator $\hat{h}_1$ described the motion of electron i in field of all nuclei.

$$\hat{h}_i = -\frac{1}{2}\nabla_i^2 - \sum_{k}^{M} \frac{Z_k}{|\mathbf{r}_k - \mathbf{r}_i|} \tag{3.9}$$

The operators $\hat{J}_i$ and $\hat{K}_i$ are the Coulomb and exchange operators respectively,

$$\hat{J}_i \phi_k (\vec{\mathbf{r}}_1) = \int \frac{|\phi_i (\vec{\mathbf{r}}_2)|^2}{|\vec{\mathbf{r}}_2 - \vec{\mathbf{r}}_1|} d\vec{\mathbf{r}}_2 \phi_k (\vec{\mathbf{r}}_1) \tag{3.10}$$

$$\hat{K}_i \phi_k (\vec{\mathbf{r}_1}) = \int \frac{\phi_i^* (\vec{\mathbf{r}}_2)\, \phi_k (\vec{\mathbf{r}}_2)}{|\vec{\mathbf{r}}_2 - \vec{\mathbf{r}}_1|} d\vec{\mathbf{r}}_2 \phi_i (\vec{\mathbf{r}}_1) \tag{3.11}$$

These equations can also be solved according to the self-consistent (SCF) procedure, where the operators are generated with a suitable choice of orbitals, and solving the equations lead to a new set of orbitals. This procedure can be repeated until the input and output orbitals differ no more up to a certain numerical accuracy. While the HF method is significantly more accurate than the previous Hartree method, it comes at poor scaling (N^4) as it requires calculations of additional many-body integrals.

3.1.3 Restricted and Unrestricted Hartree Fock

In case of closed-shell systems, since the orbitals are evenly occupied, the α- and β- spin electrons can be constrained to the same spatial orbital. Such a treatment of the wave-functions is called the *Restricted Hartree-Fock* (RHF).

When dealing with systems having odd number of electrons, RHF cannot be used therefore an extension of the RHF, called the *Restricted open-shell Hartree-Fock* (ROHF)[63] is usually considered. In ROHF, the constraints are applied to the doubly occupied orbitals while the unpaired electrons are described using singly-occupied orbitals. However, the constraints imposed in ROHF can largely deviate from the ground state.

To counter this, the *Unrestricted Hartree-Fock*[64] (UHF) is usually preferred. As the name suggests, UHF doesn't assume any variational constraints on the wave function and treats the α and β spatial orbitals independently. One drawback of UHF is that it leads to the so called *spin-contamination* i.e. the wave-functions are no longer pure-spin states and eigenfunctions of the $\mathbf{S^2}$ operator. In the cases where spin-contamination is large, there are several techniques to tackle the spin-contamination problem.[65, 66] A schematic to highlight differences between these formalisms is presented in Fig. 3.1

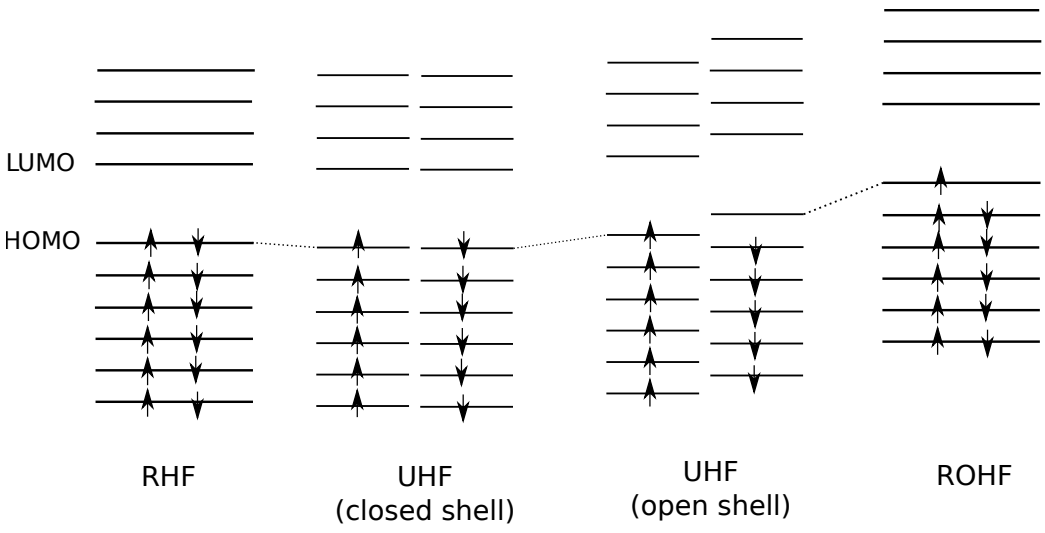

Figure 3.1: Relative energy levels of closed-shell and open-shell systems for restricted and unrestricted approaches.

3.2 Basis Sets

Almost all of the electronic structure theory concerning molecular systems uses linear combination of atomic orbitals (LCAO) to construct the molecular orbitals (MO). In other words, it is the superposition of the atomic orbitals that gives rise to MO, as represented in the following equation.

$$\phi_i = \sum_j c_{ij}\chi_j \tag{3.12}$$

where, χ_j are the AOs, and c_{ij} are the corresponding coefficients. As we have seen from the description of wave-function approximations described above, the choice of orbitals is crucial for the accuracy of the system and is dependent on the type of system which one is dealing. For example, periodic plane-waves might be a better choice of solid-state systems where electrons are only partially bound to the nuclei, atomic orbitals are usually suitable for most molecular systems where the electrons are strongly confined within the nuclear potential. Therefore, the basis functions should be able to capture the physics of the problems with minimum number of parameters and should form a complete basis-set where the generality can be maintained across different systems. Like most computational problems, this comes down to maintaining a balance between accuracy, scalability and transferability. A larger basis set can be transferable and lead to more accurate predictions but is computationally intensive.

Gaussian type orbitals

In several quantum chemistry codes, it has been a standard to represent the AOs in form of Gaussian-type basis functions. This could either be in the Cartesian or the spherical coordinate system as follows

$$\begin{aligned} \chi_{\zeta,l_x,l_y l_z}(x,y,z) &= N x^{l_x} y^{l_y} y^{l_z} \mathrm{e}^{-\zeta r^2} \\ \chi_{\zeta,n,l,m}(r,\theta,\phi) &= N Y_{l,m}(\theta,\phi) r^{2n-2-l} \mathrm{e}^{-\zeta r^2} \end{aligned} \tag{3.13}$$

where $Y_{l,m}$ are the spherical-harmonics, n, l and m are the principle, azimuthal, and magnetic quantum numbers. The Gaussian functions, $e^{-\zeta r^2}$ give the shape to the AOs where r is the radial distance to the atomic nucleus, of a single or several exponents ζ ('zetas'). The size of the basis-set is usually defined by the number of Gaussian functions used to define one AO,

e.g., minimal basis set i.e., one Gaussian function per AO would be termed as a single-zeta.

In some cases when the system is charged, the natural extent of localization of the orbitals might vary therefore additional 'polarized' or 'diffused' functions might need to be added.

3.3 Density Functional Theory

In the previous sections it was discussed that wave-functions theory such as the HF scale poorly as the number of variables rise exponentially with increasing number of electrons. Moreover, in order to incorporate the electron-correlation effects, one needs to resort to other approaches such as configuration interaction (CI) which are even more computationally expensive.

An alternative branch of *ab initio* techniques is formulated in terms of the electron-density instead of the wave-function. It counters the scaling problem to a large extent. For a system with N electrons, wave-function is a function of $3N$ coordinates (excluding spin) whereas, the density is dependent on only 3 coordinates, independent of the number of electrons.

$$n(\mathbf{r}) = N \int d^3r_2 \int d^3r_3 ... \int d^3r_N \Psi^*(\mathbf{r}, \mathbf{r_2}, ...\mathbf{r_N})\Psi(\mathbf{r}, \mathbf{r_2}....\mathbf{r_N}) \tag{3.14}$$

The idea was first introduced by Thomas[67] and Fermi[68] where they presented a formalism to calculate atomic properties using only the electron-density as the variable. The idea was further developed by Hohenberg and Kohn [69, 70] in form of two H-K theorems. First theorem states that that any ground-state property can be uniquely identified as a functional of the electron density in position space. This essentially means that once the ground-state electron density is known for the system, it can be used to calculate any property.

Furthermore, in the second HK theorem, they proved that this energy functional obeys the variational principle. Therefore, the initial guess for the electron-density can be improved by minimizing the energy functional, similar to the HF theory. Thus, assuming that the *exact* density of the system is $n(\vec{\mathbf{r}})$, the total energy can therefore be written as,

$$E_e = T[\rho(\vec{r})] + \int V_{\text{ext}}(\vec{r})\rho(\vec{r})d\vec{r} + \int V_{\text{C}}(\vec{r})\rho(\vec{r})d\vec{r} + E'_{\text{xcl}}[\rho(\vec{r})] \tag{3.15}$$

where the terms on the RHS represent the functionals corresponding to kinetic energy, external potential, Coulomb repulsion and the exchange-correlation energies respectively.

If we assume that there exists a fictitious system of non-interacting particles with same density and energy as the real system, it would give rise to a different effective potential, $V_{eff}(\vec{r})$, which could then be written as a functional derivative,

$$V_{\text{eff}}(\vec{r}) = \frac{\delta T}{\delta \rho} - \frac{\delta T_0}{\delta \rho} + V_{\text{ext}}(\vec{r}) + V_{\text{C}}(\vec{r}) + \frac{\delta E'_{\text{xc}}}{\delta \rho} \tag{3.16}$$

where the T_0 corresponds to the kinetic-energy of the fictitious system. In equation 3.16, the Coulomb and external potential are known but there is no way to know the exact nature of other terms, which is the so-called exchange-correlation potential,

$$V_{\text{xc}}(\vec{r}) \equiv \frac{\delta T}{\delta \rho} - \frac{\delta T_0}{\delta \rho} + \frac{\delta E'_{\text{xc}}}{\delta \rho} \tag{3.17}$$

The equations described above represent the Kohn-Sham DFT[70] as is used in all modern DFT codes.

3.3.1 Jacob's Ladder: Exchange-correlation Functionals

It was discussed in previous sections that Hartree-Fock (HF) based formalisms consists of a single Slater determinant. While that accounts for most of the energy, it doesn't include correlation effects. Correlation energy is the difference between the HF energy and the lowest possible energy obtained from HF for a given basis set. In order to incorporate correlation effects in wave-function methods, a linear combination of multiple Slater determinants corresponding to different electronic configurations must be considered. This is the basis for advanced quantum chemistry methods such as the configuration interaction (CI) and multireference methods which are beyond the scope of this work.

As noted above, within the density functional formalism, this can be treated using an approximate exchange-correlation functional. While the first HK theorem proves the existence of a functional, there is no systematic way to define the XC functional exactly. This still remains a challenge to

all modern DFT problems. There are several hundred approximations that exist in form of different XC functionals which can be chosen depending on the chemical system one is dealing with.

Perdew proposed a *'Jacob's ladder'* strategy to approach different XC functionals where each rung of the ladder represents one level of approximations with increase in accuracy up the ladder. The lowest rung was suggested as the local density approximation (LDA) with the assumption of density as a homogeneous electron gas and XC energy depends only on the density in the point in space, hence it's a strictly local approximation.

$$E_{\mathrm{xc}}^{\mathrm{LDA}}[n] = \int d^3\mathbf{r}\ n(\mathbf{r})\epsilon_{\mathrm{xc}}(n(\mathbf{r})) \tag{3.18}$$

where the ϵ_{xc} is the xc-energy of the electron gas.

On the next rung is the generalized gradient approximation (GGA). These functionals additionally depend on the gradient of the density at each point. Hence, this approximation is computationally expensive compared to LDA but significantly accurate.

$$E_{\mathrm{xc}}^{\mathrm{GGA}}[n] = E_{\mathrm{xc}}^{\mathrm{LDA}}[n] + \int d^3\mathbf{r}\Delta\epsilon_{\mathrm{xc}}(n, |\nabla n|) \tag{3.19}$$

PBE[71] and BLYP[72, 73] are some of the most popular GGA XC functionals.

Third rung of the ladder include the meta-GGA functionals, which in addition to local density and the gradient, also depends on the Kohn-Sham kinetic energy density, i.e. a further higher-order derivative of the electron density ($\nabla^2 n(\vec{\mathbf{r}})$). TPSS[74] is a popular example of meta-GGA functional.

Next to the meta-GGAs are the hybrid-functionals, which mix some part of GGA with an additional HF exchange energy thereby eliminating a fraction of the self-interaction present in the (semi-)local approximation on which they are based. This is a significant advantage in many systems, in particular light organic molecules. PBE0[75] and B3LYP[76] are quite often used.

The choice of the xc-functional largely depends on the kind of system and the properties one is interested to calculate. However, as all functionals are approximations, there is an inherent delocalization error that is one of the roots of major failures of DFT causing inaccurate predictions of several material properties. Due to the delocalization error the electron density falsely tends to over delocalize depending on the nature of approximation used in the functional. This is a major reason why DFT tends to underestimate the

band gap. For this reason, hybrid functionals are generally recommended for molecular systems as they tend to have some sort of error cancellation as they incorporate HF approximation to a certain extent.[77]

Chapter 4

Modeling the spin-admixture parameter

4.1 Theory

Spin-orbit coupling (SOC) is one of the major factors of spin-relaxation. Therefore, an accurate and general description of SOC operator from first principles is essential.

This chapter begins by describing Zeroth Order Regular Approximation (ZORA), which is widely used approximation to describe SOC in molecular systems. Then, a generalized formalism is presented γ to remove all limitations on predictive accuracy and transferability between different systems inherent in the original formulation.[39] Finally, the performance of this method is compared against the original formulation by using the model systems, while exploring the influence of computational variables such as the electronic exchange-correlation approximations on γ, as described in Section 4.1.3. All results and a discussion of the same are presented in Section 4.2.

4.1.1 SOC from First principles: Zeroth Order Regular Approximation (ZORA)

SOC plays an intricate role in most of the spin-relaxation mechanisms discussed previously. Therefore our goal is to get an accurate description of the SOC operator from first principles. The fundamentals of electronic structure theory discussed in chapter 3 were in the non-relativistic limit. However,

since SOC is a relativistic effect we take it a step further. Our starting point is the time-independent Dirac equation.

$$\left[c\boldsymbol{\alpha}\cdot\mathbf{p}+\boldsymbol{\beta}'mc^2+\mathbf{V}\right]\Psi=E\Psi \tag{4.1}$$

where $c\alpha$ (c = speed of light) and β can be expressed in form of 4×4 matrices where the former consists of the Pauli spin matrices and the latter as a block diagonal unitary-matrix.

Directly solving the four-component Dirac equation 4.1 is computationally unfeasible for large systems. Several approaches involve assuming the solution in form of two-components, namely the *large* and *small* components originating from the electronic and positronic degrees of freedom respectively. Since we are interested only in the electronic solutions, some kind of reduction of four-component formalism is preferred.

Some simplifications such as Pauli-like Hamiltonians[78] use a similar approach, however, they suffer from a singularity close to the nucleus due to the Coulomb like nature of the potential.

Another feasible two-component approach is called the Zeroth order regular approximation (ZORA). The ZORA equation can be obtained by solving the Dirac equation for the large component and expanding the relativistic operator in zeroth order under the condition where $E/(m_ec^2-V)<1$.[79] Doing so avoids the divergence close to nucleus and remains true for the chemical systems. Finally we can write the complete ZORA Hamiltonian as follows:

$$H^{ZORA}\Psi=\left[\mathbf{V}+\mathbf{p}\frac{c^2}{\left(2c^2-\mathbf{V}\right)^2}\mathbf{p}-\frac{c^2}{2c^2-V}\mathbf{s}\cdot(\nabla\mathbf{V}\times\mathbf{p})\right]\Psi=E\Psi \tag{4.2}$$

$$H^{ZORA}=H_{SR}^{ZORA}+H_{SO}^{ZORA} \tag{4.3}$$

The two terms in the ZORA Hamiltonian represents the scalar-relativistic and fully-relativistic corrections and V is the total electronic potential. This Hamiltonian is general, accurate and directly obtainable from first-principles. Now that we have defined the SOC operator, we'll use it in defining the spin-admixture.

4.1.2 Generalization of spin-admixture parameter

The dominant single-electron term of the Breit-Pauli[78, 80] SOC operator in atomic units can be written as

$$\begin{aligned}\hat{H}_{soc} &= \frac{\alpha^2}{2}\sum_{i,k}(\frac{Z_k}{r_{ik}^3}\hat{\mathbf{r}}_{ik}\times\hat{\mathbf{p}}_i)\cdot\hat{\mathbf{s}}_i = \frac{\alpha^2}{2}\sum_i \xi_i\hat{\mathbf{l}}_i\cdot\hat{\mathbf{s}}_i \\ &= \frac{\alpha^2}{4}\sum_i \xi_i \begin{bmatrix}\hat{\mathbf{l}}_i^z & \hat{\mathbf{l}}_i^- \\ \hat{\mathbf{l}}_i^+ & -\hat{\mathbf{l}}_i^z\end{bmatrix}, \hat{\mathbf{l}}^{+(-)} = \hat{\mathbf{l}}^x + (-)i\hat{\mathbf{l}}^y\,,\end{aligned} \tag{4.4}$$

where α is the fine structure constant, $\hat{\mathbf{r}}_{ik}$ is the separation vector to atomic nucleus k of effective charge Z_k, $\hat{\mathbf{p}}_i$ is the momentum and $\hat{\mathbf{s}}_i$ is the spin-angular momentum for the ith electron. The atomic spin-orbit (SO) constants ξ_i provide the nuclear Coulomb potential scaling of orbital angular momentum $\hat{\mathbf{l}}_i$ relative to the atomic nuclei for electron i. In the last step, $\hat{H}_{soc}$ is written in the Pauli spin basis. Expectation values of $\hat{\mathbf{l}}^z$ ($\hat{\mathbf{l}}^{+/-}$) are non-zero for orbital pairs of same (opposite) spin.

As the spin-orbit corrections are small for organic molecules, the spin-mixed density-functional theory (DFT) wave-functions ($|\psi_0+\rangle$) can be written according to first-order perturbative expansion as follows

$$\begin{aligned}|\psi_0+\rangle &= |\psi_0\uparrow\rangle - \sum_{k\neq 0\sigma}\frac{\langle\psi_k\sigma|\sum_i \xi_i\hat{\mathbf{l}}_i\cdot\hat{\mathbf{s}}_i\,|\psi_0\uparrow\rangle}{E_k-E_0}\,|\psi_k\sigma\rangle \\ &= |\psi_0\uparrow\rangle - \sum_{k\neq 0}\frac{1}{2}\Bigg[\frac{\langle\psi_k\uparrow|\sum_i \xi_i\hat{\mathbf{l}}_i^z\,|\psi_0\uparrow\rangle}{E_k-E_0}\,|\psi_k\uparrow\rangle \\ &\quad - \frac{\langle\psi_k\downarrow|\sum_i \xi_i\hat{\mathbf{l}}_i^-\,|\psi_0\uparrow\rangle}{E_k-E_0}\,|\psi_k\downarrow\rangle\Bigg]\,,\end{aligned} \tag{4.5}$$

where $|\psi_k\rangle$ are the orbitals of the SO-free Hamiltonian, and E_k are the corresponding orbital energies obtained from restricted open-shell Kohn-Sham (ROKS) electronic structure calculations. σ and i are summations over spins and orbitals, respectively. The ROKS approximation represents a very significant variational constraint on the Kohn-Sham wave-function compared to the unrestricted (UKS) approximation.

The spin-admixture parameter can be calculated as a difference from the norm of the perturbed and the SO-free states.

$$\langle\psi_0+|\psi_0+\rangle = \langle\psi_0\uparrow|\psi_0\uparrow\rangle + \gamma^2 = 1 + \gamma_{\uparrow\uparrow}^2 + \gamma_{\uparrow\downarrow}^2\,, \tag{4.6}$$

where γ^2 is the sum of mixing between same- ($\gamma^2_{\uparrow\uparrow}$) and opposite ($\gamma^2_{\uparrow\downarrow}$) spin orbitals, arising from the $\hat{\mathbf{l}}^z$ and $\hat{\mathbf{l}}^{+/-}$ operators, respectively. The subscript 0 indexes the spin-carrying orbital.

In Ref. [39], the unknown SO constants ξ_i are approximated by mapping experimental measurements of atomic orbitals (AOs) up to p angular momentum onto the matrix elements of Eq. 4.5. From a DFT perspective, it is only possible with a minimal basis set i.e. using one AO per basis function. In addition to the ROKS constraint, the approach is semi-empirical and leads to a poor description of the molecular orbitals. The limitation to p-basis functions also restricts the technique to calculations on molecular π-orbitals, and consequentially, to light organic molecules only.

First step of modifications is generalization of Eq. 4.5 to the UKS approximation for which the approach adopted by Neese and Solomon,[81] is used. The eigenvalues in the denominator of Eq. 4.5 ($E_k \rightarrow E_{k\uparrow}\,/\,E_{k\downarrow}$) are spin-labelled and the corresponding energies are calculated from UKS approximation.

Secondly, the SOC operator is calculated using the zeroth order regular approximation[79] (ZORA) to the fully-relativistic Dirac equation[22] instead of using semi-empirical SOC constants. The fully-relativistic SOC matrix elements in Eq. 4.3 are then treated as perturbation to the wave-functions calculated at scalar-relativistic level of theory. The spatial matrix elements of $\hat{H}^{ZORA}_{SO}$ from Eq. 4.2 in the atomic-orbital basis are[79]

$$\hat{L}^l_{ij} = i \sum_{mn} \epsilon_{lmn} \left\langle \frac{\partial \psi_i}{\partial x_m} \middle| \frac{V}{4c^2 - 2V} \middle| \frac{\partial \psi_j}{\partial x_n} \right\rangle , \tag{4.7}$$

where the permutation matrix ϵ_{lmn} is the Levi-Civita tensor and x_m is the Cartesian basis. The matrix elements $\hat{L}^l_{ij}$ are scaled by effective SO constants, thereby, inheriting the first-principles qualities of V.

The matrix elements in Eq. 4.7 are transformed to the molecular orbital (MO) basis, and substituted into Eq. 4.5. The mixed spin-carrying orbital can be written as

$$|\psi_0 +\rangle = |\psi_0 \uparrow\rangle + \sum_{k\neq 0} [a_k \, |\psi_k \uparrow\rangle + b_k \, |\psi_k \downarrow\rangle] \, , \tag{4.8}$$

where,

$$\begin{aligned} a_k &= \frac{1}{2}\frac{\langle \psi_k \uparrow | \hat{L}^z | \psi_0 \uparrow \rangle}{E_{k\uparrow} - E_0} \\ \text{and } b_k &= \frac{1}{2}\frac{\langle \psi_k \downarrow | (\hat{L}^x + i\hat{L}^y) | \psi_0 \uparrow \rangle}{E_{k\downarrow} - E_0} \,. \end{aligned} \tag{4.9}$$

Here, $\hat{L}^{x,y,z}$ are the full matrices of Eq. 4.7. Note the spin-labeled eigenvalues ($E_{k\downarrow}$ / $E_{k\uparrow}$) for UKS.

Finally, substituting Eq. 4.9 into Eq. 4.8, and further into Eq. 4.6,

$$\gamma^2 = \sum_{k\neq 0} [a_k^* a_k + b_k^* b_k] \tag{4.10}$$

This re-derivation of γ using a more accurate approximation of the effective SOC potential is independent of any restrictions imposed by the use of atomic SOC constants and enables use of a larger basis set. It is worth mentioning that ZORA is only one of the approximations to SOC operator and this derivation can be easily extended to other similar two-component approximations, such as the Douglas-Kroll-Hess [82, 83] method, that are valid at a single-determinant level of theory.

The code to calculate the spin-admixture from output of `NWCHEM` ZORA/DFT calculation can be downloaded online.[1]

4.1.3 Density functional theory calculations

The accuracy of γ is largely determined by the quality of first-principle calculations. As can be noticed from equation 4.9, γ is sensitive to the SOC matrix elements, which are governed by effective potential V, the MO wavefunctions, and their corresponding energies.

As also discussed in the chapter 3, the absence of an exact xc-functional leads to a delocalization error[77] in molecules energy levels and consequently, the properties to be poorly described. The use of hybrid functionals allow reducing some delocalization error by the addition of 'exact' non-local Hartree-Fock exchange and have proven a successful solution to this problem, from calculations of electronic-[84] and magnetic[85, 86] properties in organic molecules to light transition metal chemistry.[87]

[1] `https://github.com/UdayChopra/spin-admixture`

The influence of xc-approximations on γ is systematically explored starting from the semi-local PBE[71] functional that belongs to the generalized gradient approximation (GGA) and was also used in the original formulation in Ref. [39]. This has been compared to the PBE0[75], hybrid functional that includes 25% of exact exchange. For comparison, the fully non-local exchange used in Hartree-Fock approximation and the local density approximation (LDA) functional PW92[88] are also included.

While PBE0 minimizes the electron delocalization error there are other drawbacks inherent to the DFT that require more sophisticated techniques. One of them is the static correlation error[77] that leads to large errors in systems that contain strong-correlation effects or near-degeneracies. Such systems includes molecules containing f-electron elements that make up most of the interesting single-molecular magnets.[89, 90] These molecules lie outside the scope of this study however, some range separated hybrid functionals such as the HSE[91, 92] have been successfully employed in calculating accurate electronic structure and magnetic properties of these systems.

Computational Details

The NWChem quantum chemistry suite[93] version 6.5 for all DFT calculations within the zeroth order regular approximation (ZORA). All properties were found converged with respect to the SARC[94] all-electron, minimally augmented, polarized triple-zeta valence basis set recontracted for ZORA (a.k.a. 'MA-ZORA-Def2-TZVP'). This basis set, with the carbon atom diffuse (minimal augmentation) functions removed in order to eliminate linear dependencies, was used in all calculations unless otherwise stated.

Because of the partially very weak spin-mixing in the studied molecules, great care was taken to eliminate sources of numerical errors in the calculations: the self-consistent field (SCF) convergence and Coulomb integral screening thresholds were set at $10^{-8} - 10^{-10}$ [Ha] and 10^{-14}, respectively. Integration grids were set at the maximum ('xfine') density. SCF convergence aids such as level shifting, and initial high tolerances in the SCF cycle were turned off (options 'nolevelshifting' and 'tight', respectively). Spin contamination was negligible ($< 10\,\%$) in all UKS calculations.

All γ calculations were done on molecules fully geometry optimized in the respective charge states, at the stated level of theory, without symmetry constraints.

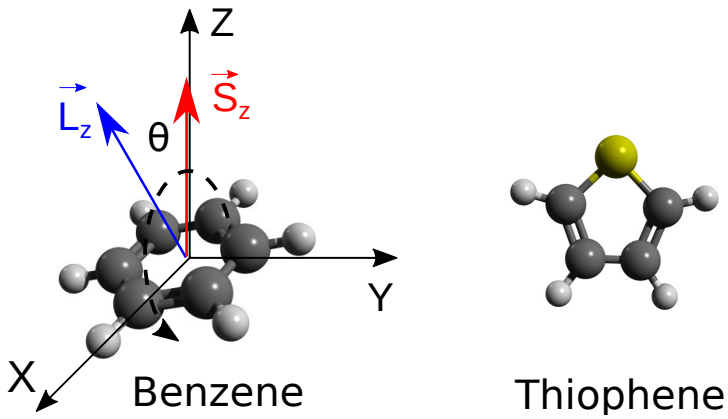

Figure 4.1: Benzene and Thiophene molecules for which the spin-admixture is calculated with an illustration of the rotation of their conjugation plane with fixed spin-quantization axis

4.2 Comparison with original formulation

We begin by computing our reformulated γ for single-ring conjugated molecules. In order to study the effects on our generalized γ of the relative orientation of orbital- and spin-angular momentum, we rotate the spin in a planar molecule. The highest occupied molecular orbital (HOMO) of benzene (C_6H_6), which has p_z orbital angular momentum, is one of the simplest possible system. Removing an electron results in a spin-1/2 system which is rotated by an angle θ through 180 degrees about the y-axis, with the spin quantization axis fixed along z. This is equivalent to rotating the spin in a stationary molecule from parallel- to anti-parallel alignment with the orbital angular momentum (see Fig. 4.1).

First the effect of the unrestricted Kohn-Sham (UKS) vs. restricted open shell Kohn-Sham (ROKS) approximations on γ is isolated using the PBE xc-functional, the 'STO-6G' Slater-type minimal basis set, and the SOC approximation and empirical ξ_i as in Ref. [39]. This is shown in Fig. 4.2. The ROKS results are quantitatively very close and qualitatively identical to those of Ref. [39]. The ROKS γ^2 (blue solid line) is constant with the rotation angle θ. The reason is the orbital symmetry of the ROKS canceling the changes in the opposite- ($\gamma^2_{\uparrow\downarrow}$, dashed blue line) and same-spin ($\gamma^2_{\uparrow\uparrow}$, dotted blue line) contributions to γ^2. This is a consequence of degenerate energy

levels for up- and down-spin molecular orbitals. This is obviously incorrect, since properties proportional to the absolute magnitude squared of the $\hat{\mathbf{l}} \cdot \hat{\mathbf{s}}$ scalar product (Eq. 4.4) should resemble a $cos^2(\theta)$ curve.

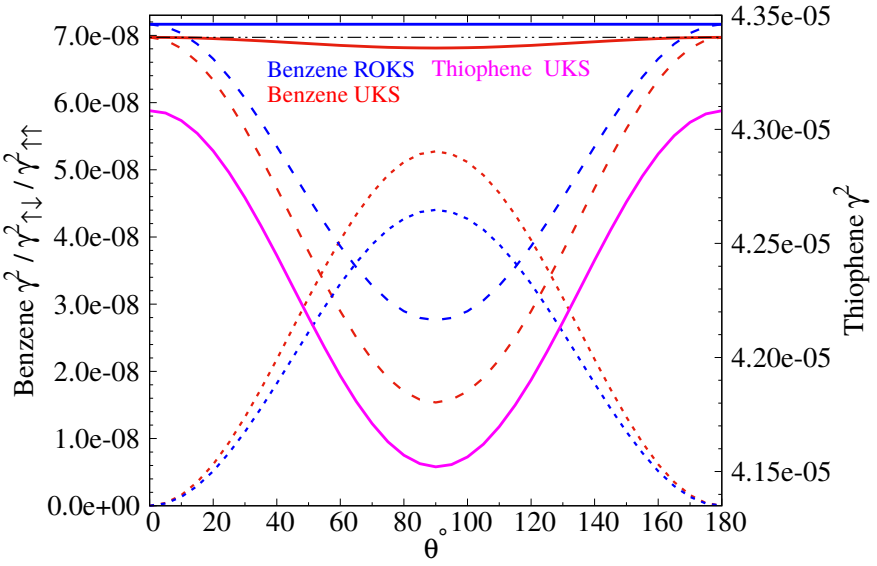

Figure 4.2: γ^2 as a function of the angle of plane of conjugation with quantization axis for Benzene and Thiophene molecule for PBE functional at UKS and ROKS level of theory using a minimal basis set.

Repeating the calculation using the UKS approximation (solid red line) breaks the degeneracy between opposite-spin orbitals and the resulting curve is as expected although weakly for benzene.

Next, we examine the effect of electron delocalization error on the benzene $\gamma^2(\theta)$ curves, by recomputing with the above level of theory, but different exchange-correlation (xc) approximations (see Fig. 4.3). The $\gamma^2(\theta)$ curves stay qualitatively the same, but quantitatively reduce by almost a factor of three from a fully local (LDA/PW92) via a hybrid (PBE0) to a fully non-local (Hartree-Fock, HF) xc-approximation, for both positive (solid lines) and negative charges (dashed lines). The LDA curve in Fig. 4.3 is nearly identical to that of GGA/PBE in Fig. 4.2. The high γ for the (semi-)local functionals is due to underestimated orbital energy differences in the denominator of Eq. 4.9, caused by electron delocalization error. However, since the HF approximation induces the opposite error,[77] the best estimate of γ

lies between the LDA/GGA and HF extremes. Therefore, while the exact solution is unknown, the hybrid PBE0 xc-functional is closest to it.

From here on, we employ the ZORA/UKS/PBE0 level of theory with a TZVP basis set (see Section 4.1.3) in all calculations. In the simple benzene system, the only effect of this improvement is an overall shift of the curves in Figures 4.2 and 4.3.

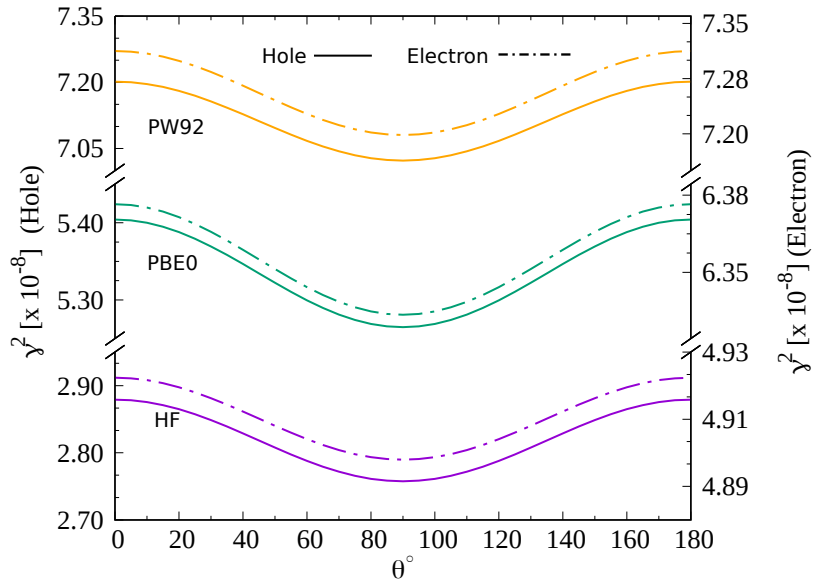

Figure 4.3: The UKS γ^2 curve of Fig. 4.2 repeated for fully local (PW92), hybrid (PBE0), and fully non-local (HF) xc approximations for cationic (solid line) and anionic (dotted-dashed line) benzene molecule.

4.3 Summary

In this chapter, a generalized formalism to calculate the spin-admixture parameter was presented. The generalizations consist of (a) using a more accurate unrestricted Kohn-Sham formalism to describe open-shell systems and (b) calculating the SOC matrix-elements from first-principles using ZORA. These refinements have led to a completely parameter free approach that allows use of an arbitrarily large basis set in DFT calculations as opposed to a minimal basis-set. This enables us to conveniently calculate spin-admixture of molecules involving molecular orbitals other than just $\pi-$orbitals.

The dependence of different xc-functionals was also explored in the calculations and it was found that spin-admixture is extremely sensitive to the delocalization error inherent in the DFT functional.

These modifications over the original formulation[39] show both qualitative and quantitative improvements as demonstrated using the example of simple planar conjugated molecules such as benzene and thiophene. In the following chapters, this new approach is used to understand behaviour of SOC in molecules that are more relevant to spintronic applications and would also focus on how crucial the spin-admixture is to understand the spin-relaxation in those molecules.

Chapter 5

Tuning the molecular spin-admixture

Organic compounds offer several possibilities to chemically tune physical properties via synthesis. The goal of this chapter is to explore how the chemical composition and molecular structure influence the γ and hence the spin-orbit coupling (SOC) using molecules of interest as an example. Through this discussion, it will also be emphasized that the approach is transferable across different classes organic molecules. Finally, the theory is benchmarked against recent experiments[21] on spin-transport in high-mobility polymers underlining the significance of γ in understanding and tuning spin-relaxation.

A common rule of thumb to compare SOC between different compounds is via the atomic number (or weight) of elements. Atomic SOC is often assumed to be proportional to Z^4, where Z is the atomic number of constituent element. However, this does not necessarily hold true for γ. To demonstrate this, γ is calculated for several compounds belonging to different classes of organic semiconductors that are relevant to spintronics. These molecules are presented in Fig. 5.1 and the values of spin-admixtures are listed in table 5.1.

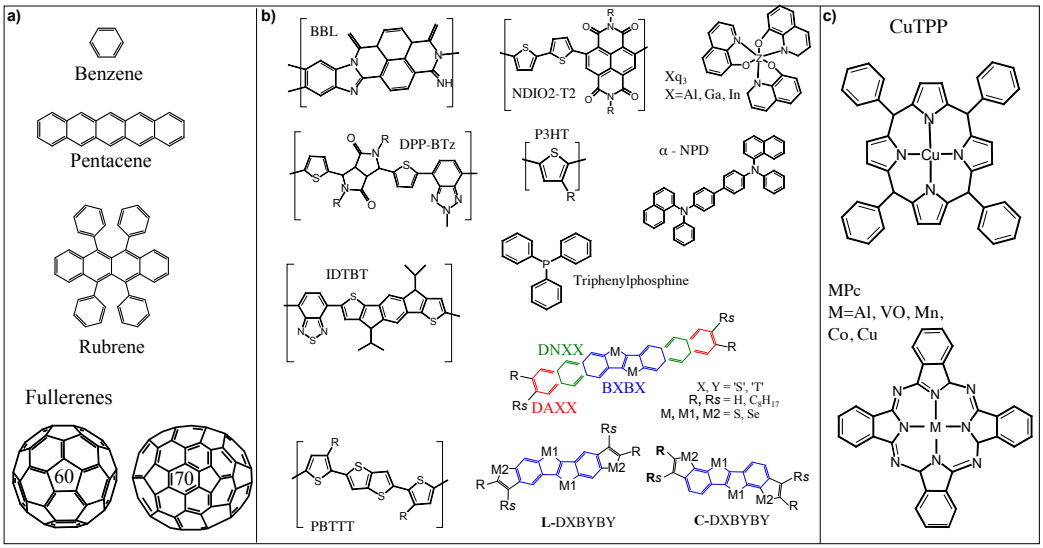

Figure 5.1: Chemical structures for which γ^2 calculations are performed. (a) Aromatic hydrocarbons. (b) Hetero-atomic π-conjugated polymers and molecules (c) Transition metal complexes of phthalocyanine and tetraphenyl-porphyrins.

As can be observed from Fig. 5.1, the molecules are divided into three classes (a) aromatic hydrocarbons, (b) heteroatomic $\pi-$conjugated systems and (c) transition metal complexes.

Most of the lightweight and heteroatomic π-conjugated systems such as the pentacene and rubrene are known for their high-mobilities and have demonstrated magnetoresistance effects in organic spin-valves[53, 95, 96]. Chalcogenide polymers like PBTTT, P3HT, IDTBT etc., share similar high-mobility characteristics[97–101] and are of special interest in the spintronics due to recent studies on long spin-diffusion length and inverse-spin Hall effect.[102, 103] Furthermore, they allow a vast range of possibilities for tuning SOC with chemical modifications such as substitution with heavier elements or modifying the alkyl chains.[104, 105] Complex π-conjugated molecules like tris-(8-hydroxyquinolinato)aluminium (Alq_3), although possessing a low mobility of $10^{-5}cm^2V^{-1}s^{-1}$ is an interesting systems as it contains a metal center in addition to $\pi-$conjugated ligands. It was one of the first molecules to be used in spintronic devices[19, 106] and has been widely studied since then.[40, 41, 107]

Another class considered here is that of metal-complexes that are of primary importance in the field of molecular magnetism. The goal of studying them is to bridge the gap between conventional organic semiconductors and single-molecule magnets (SMM) based spintronics. Metal complexes included in study are with phthalocyanine (Pc) and tetraphenylporphyrin (TPP) ligands. The list attempts to include representative molecules from all different classes of organic semiconductors to study behavior of SOC across different systems. Using these molecules, the effect of elemental composition and structure on γ will be discussed.

It should be emphasized here that g-tensor shifts (Δg) is another widely-used measure of SOC. Since the relationship between these two quantities is not relevant to the following discussion it is discussed in detail in Appendix A.

Molecule	γ^2	**Molecule**	γ^2
Aromatic hydrocarbons		DASS	$4.85 \cdot 10^{-5}$
Benzene	$2.36 \cdot 10^{-8}$	C8-DASS	$4.42 \cdot 10^{-5}$
Pentacene	$2.69 \cdot 10^{-8}$	C8s-DASS	$4.74 \cdot 10^{-5}$
Rubrene	$3.85 \cdot 10^{-8}$	*CDSBTBT	$1.16 \cdot 10^{-4}$
C_{60}	$5.89 \cdot 10^{-8}$	*C8-CDSBTBT	$9.34 \cdot 10^{-5}$
C_{70}	$7.81 \cdot 10^{-8}$	*C8s-CDSBTBT	$1.22 \cdot 10^{-4}$
Heteroatomic π-conjugated		LDSBTBT	$1.12 \cdot 10^{-4}$
α-NPD	$8.10 \cdot 10^{-8}$	C8-LDSBTBT	$1.24 \cdot 10^{-4}$
Tri-phenylphosphine	$5.29 \cdot 10^{-7}$	C8s-LDSBTBT	$1.15 \cdot 10^{-4}$
Alq_3	$8.49 \cdot 10^{-5}$	*CDSBSBS	$1.47 \cdot 10^{-4}$
Gaq_3	$7.37 \cdot 10^{-5}$	*C8-CDSBSBS	$1.01 \cdot 10^{-4}$
Inq_3	$3.81 \cdot 10^{-5}$	*C8s-CDSBSBS	$1.09 \cdot 10^{-4}$
BTBT	$4.39 \cdot 10^{-6}$	LDSBSBS	$1.76 \cdot 10^{-4}$
C8-BTBT	$2.53 \cdot 10^{-6}$	C8-LDSBSBS	$1.90 \cdot 10^{-4}$
C8s-BTBT	$4.22 \cdot 10^{-6}$	C8s-LDSBSBS	$1.62 \cdot 10^{-4}$
DNTT	$2.03 \cdot 10^{-6}$	PBTTT	$3.15 \cdot 10^{-7}$

C8-DNTT	$1.70 \cdot 10^{-6}$	P3HT	$3.68 \cdot 10^{-7}$
C8s-DNTT	$1.67 \cdot 10^{-6}$	NDI-T2	$8.73 \cdot 10^{-7}$
DATT	$1.35 \cdot 10^{-6}$	IDTBT	$1.71 \cdot 10^{-7}$
C8-DATT	$1.23 \cdot 10^{-6}$	DPPBTz	$5.29 \cdot 10^{-7}$
C8s-DATT	$1.32 \cdot 10^{-6}$	BBL	$2.44 \cdot 10^{-7}$
*CDTBTBT	$3.53 \cdot 10^{-6}$	*C8-BSBS	$1.12 \cdot 10^{-4}$
*C8-CDTBTBT	$1.38 \cdot 10^{-6}$	*C8s-BSBS	$1.64 \cdot 10^{-4}$
LDTBTBT	$5.09 \cdot 10^{-6}$	**Single molecular magnets**	
C8s-LDTBTBT	$4.63 \cdot 10^{-6}$	AlPc	$9.30 \cdot 10^{-8}$
C8-LDTBTBT	$6.15 \cdot 10^{-6}$	VOPc	$6.20 \cdot 10^{-6}$
BSBS	$1.11 \cdot 10^{-4}$	MnPc	$2.41 \cdot 10^{-2}$
DNSS	$7.28 \cdot 10^{-5}$	CoPc	$5.70 \cdot 10^{-3}$
C8-DNSS	$6.18 \cdot 10^{-5}$	CuPc	$3.72 \cdot 10^{-4}$
C8s-DNSS	$6.09 \cdot 10^{-5}$	CuTPP	$5.46 \cdot 10^{-4}$

Table 5.1: Spin-admixtures calculated for all the molecules in Fig. 5.1. Molecules marked with * represent outliers in the correlation plot in Fig. A.1.

5.1 Chemical Composition

The entire discussion has been summarized in Fig. 5.2 where the spin-admixture of all molecules is plotted against the atomic number of the heaviest element present in the corresponding molecule.

5.1.1 π-conjugated molecules

A molecule with heavier atoms is generally considered to have a larger SOC as compared to one with a light-weight chemical composition. In agreement with this, the light-weight aromatic hydrocarbons have the smallest γ. Following the increasing order of atomic weights, heteroatomic π-conjugated

molecules have γ in the order of nitrogen-based, followed by sulfur-based, and finally selenium-based molecules and polymers. It is also observed that in molecules with multiple chalcogens, substituting a single S with Se is sufficient for a larger γ^2. For example, DSBTBT and DSBSBS have $\gamma^2 \sim 10^{-4}$. These facts imply that spin-mixing is generally governed by the heaviest atom in the molecule and may not be significantly influenced by multiple substitutions. The variations due to an alkyl functional group are also investigated. However, no consistent trend is observed.

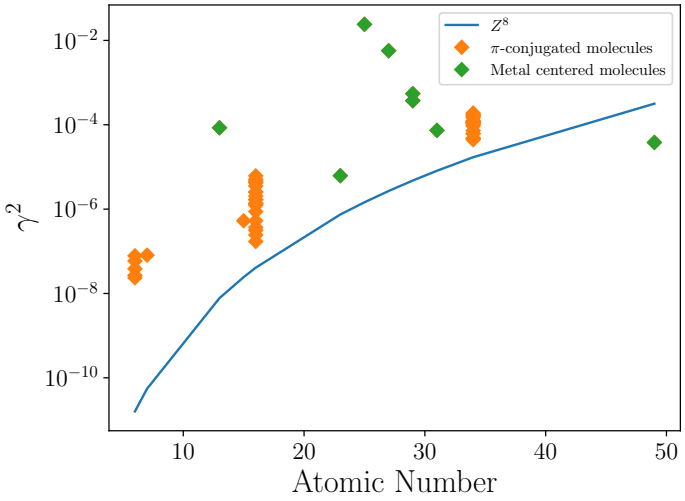

Figure 5.2: γ^2 as a function atomic number (Z) of heaviest element in the molecule. Orange points indicate the $\pi-$conjugated systems. Green points include Pc and TPP transition metal complexes and the Xq_3s. The Z^8 (blue) is shown for reference.

5.1.2 Metal-centered molecules

For the molecules mentioned above, although we see that γ, and hence the SOC, increases with heavier elements, Xq_3 and metal-complexes do not follow this rule. The γ^2 for all Xq_3 molecules lie within a range of $\sim 10^{-5}$, and does not show any variation on substituting with heavier elements. Another exception is found in the case of metal-complexes where γ^2 varies within six orders of magnitude, ranging between 10^{-8} for AlPc and 10^{-2} for MnPc.

This difference in variation for $\pi-$conjugated systems and metal com-

plexes can be reasoned based on molecular orbital (MO) where the spin is localized. The charge and hence the spin in Xq_3 molecules is present on the quinolate ligands which are π-conjugated, therefore they have little to no interaction with the higher-orbital angular momentum $d-$orbitals from the metal center. Irrespective of the substitution with a heavier element, the spin-carrying orbital is always the same and therefore we don't see any variation in the spin-admixture.

Similar reasoning can be extended to MPcs which are neutral molecules with unpaired electrons in $d-$orbitals. The spin-carrying molecular orbital for each metal complex has contribution from different $d-$orbital hybridised with the phthalocyanine ligand. Therefore, spin-admixture shows a large variation within $3d-$transition elements. Furthermore, the γ^2 for CuPc and CuTPP are quantitatively similar as it is the same spin-carrying orbital in both the cases. For AlPc, as there are no $d-$orbitals at all, the unpaired electron is present on the π-conjugated Pc ring hence it has the smallest spin-admixture in the series.

Experiments on MPcs by Bader *et al.*[108] report a similar behavior where they measure longitudinal spin-relaxation times, T_1s, at low temperature. Trying to correlate these measurements with atomic number (usually regarded measure of SOC) one would conclude that SOC does not cause spin-relaxation otherwise the T_1 of Cu should be fastest but that's not the case. In Fig. 5.3 we show a correlation between γ^2 and T_1^{-1}. The fit $\kappa = 1.73 \times 10^{-5}$ produces $T_1 \approx \frac{\kappa}{\gamma^2}$ with and RMS error of $\sim 40\%$, over four-orders of magnitude.

This strong correlation also indicates that the spin-relaxation in these molecules is driven by SOC. Although γ has been discussed in the context of a hopping-driven spin-flip mechanism, it is highly unlikely that hopping events occur at 7 K in dilute solutions. It also eliminates the presence of any spin-spin interactions.

Hyperfine interactions (HFI) play an important role in EPR transitions, therefore we performed calculations of HF field strengths at same level of theory as γ. However, in our calculations[1]. we find that the VO-, Co- Cu- and MnPc HF strengths are 39, 34, 37 and 13 [mT] respectively which fails to explain the trend in T_1s. Therefore, HFI can also be ruled out as mechanism for spin-relaxation as well.

[1]HFI calculations are performed at same level of theory as the spin-admixture using NWChem package[93]

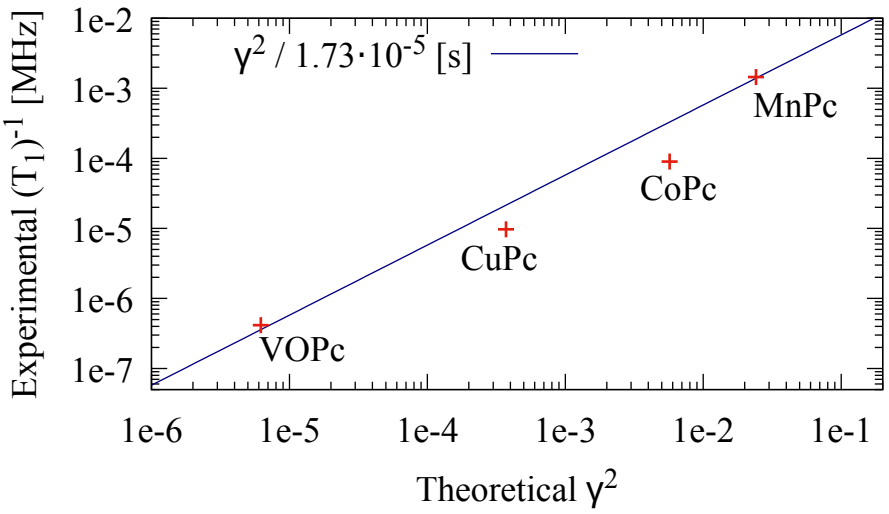

Figure 5.3: Correlation for γ^2 vs $(T_1)^{-1}$ for MPcs and the linear fit corresponding to $(T_1)^{-1} = \frac{\gamma^2}{\kappa}$

As mentioned before, spins can also couple with lattice vibrations and relax via SOC. Relaxation via spin-phonon couplings have been shown to have a identical dependence to SOC [31] i.e. $T_1 \propto H_{SOC}^2$. Therefore, a high-correlation in Fig. 5.3 is indicative of a vibration-driven spin-relaxation. It is expected that at lower temperatures, low-energy vibrational modes coupled with SOC would cause the relaxation in these molecules.

Orbital	γ^2	$(T_1)^{-1}$ [MHz][108]	T_1 Fit Error [%]
VOPc (d_{xy})	$6.20 \cdot 10^{-6}$	$4.16 \cdot 10^{-7}$	+16
MnPc (d_{yz}/d_{zx})	$2.41 \cdot 10^{-2}$	$1.45 \cdot 10^{-3}$	+5
CoPc (d_{z^2})	$5.70 \cdot 10^{-3}$	$9.01 \cdot 10^{-5}$	-61
CuPc ($d_{x^2-y^2}$)	$3.72 \cdot 10^{-4}$	$9.71 \cdot 10^{-6}$	-55

Table 5.2: From left to right: The spin-carrying orbital in the four MPc molecules (see text), the calculated γ^2 value of these orbitals, the inverse of T_1 for each MPc measured in D_2SO_4 solution at 7 K[108], and the error to experiment of T_1 approximated on the form $T_1 \approx \frac{\kappa}{\gamma^2}$ (see text).

5.2 Molecular structure and geometry

Electronic structure of molecules is highly sensitive to variations in their geometry and directly influences the SOC. In most high-mobility polymers, dihedral angles between conjugated units is a major source of these fluctuations. The variation of spin-mixing w.r.t the dihedral angles (ϕ) between two adjacent $\pi-$orbitals was derived by Yu [39] as $\gamma^2 = \gamma_0^2(1+tan^2\phi)$, where γ_0^2 is the spin-admixture for perfectly aligned orbitals.

This can be seen in Fig. 5.4 for a biphenyl molecules which is the simplest possible representation of such a system. This behavior is attributed to the effect of the angular momentum operator, which gives a zero expectation value when the adjacent $\pi-$orbitals are parallel; however, with increased torsion angles, the overlaps between opposite-spin orbitals also increase. Similar variation is also described for a polyacetylenes.[31]

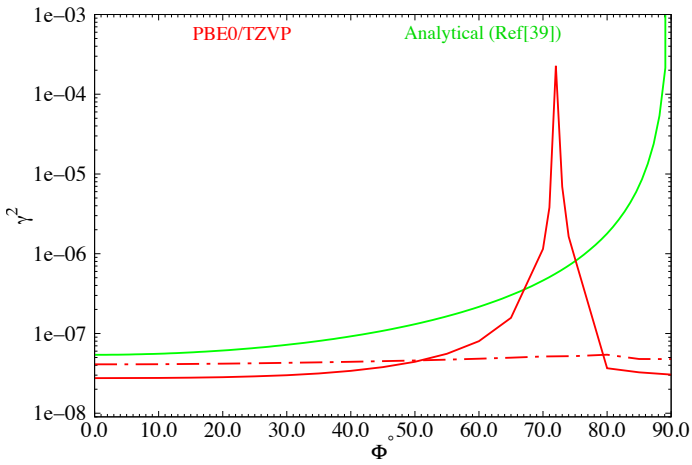

Figure 5.4: Variation of γ^2 for a charged biphenyl molecule w.r.t the dihedral angle between two units of the molecule. Solid (dashed) lines indicate positive (negative) biphenyl ions.

Long chained polymers in which the individual units are connected via C-C single bonds have a large degree of freedom in the torsional angles between monomers. Subtle fluctuations in the structure can lead to vastly different SOC strength which can cause considerable variation in observable properties. For a multiscale treatment of a realistic organic morphology, the parameters relevant to spin-transport would have to be calculated for all the

segments.

In Fig. 5.5 we present a distribution of γ^2 calculated for relevant polymer systems such as PBTTT, NDIO2-T2 and IDTBT. The calculations were performed on hundreds of segments obtained from polymer morphologies simulated using molecular dynamics. The polymers are usually found in semi-crystalline structures and have a certain degree of disorder as described above. These details in the micro-structure are consequentially encapsulated in the distribution.

From Fig. 5.5 we can make several inferences about the spin-transport in these polymers. Firstly, it is apparent that the values of γ^2 for planar segments are smallest compared to their corresponding distribution because of absence of any kind of disorder. Also, since the chemical composition of the polymers are almost similar, the values of γ^2 don't vary significantly for a crystalline geometry.

Secondly, we observe that while the average value of distributions are similar, the width is vastly different for amorphous morphologies due to a larger degree of variation in the dihedral angles between the individual units. For example, the NDIT2- and O2- units are bulkier and tend to have dihedral angles close to and sometimes larger than 40° which corresponds to the outliers in the distribution. The distribution also reveals which sites are more likely to cause a larger spin-relaxation in a stochastic spin-dynamics simulation, however this would also require an in-depth analysis of hopping rates and occupation probabilities for these sites which is beyond the scope of this work.

Large distortions along the backbone in amorphous phase may also cause the charge being localized over a smaller unit. This also affects the spin-mixing. We further investigate the effects of charge delocalization on spin-mixing by varying the number of monomers in the polymer chain for IDTBT, as summarized in the table 5.3. Since the value does not change beyond four units so as to affect the distribution in Fig. 5.5, that is selected as size of a polymer segment to save computational costs.

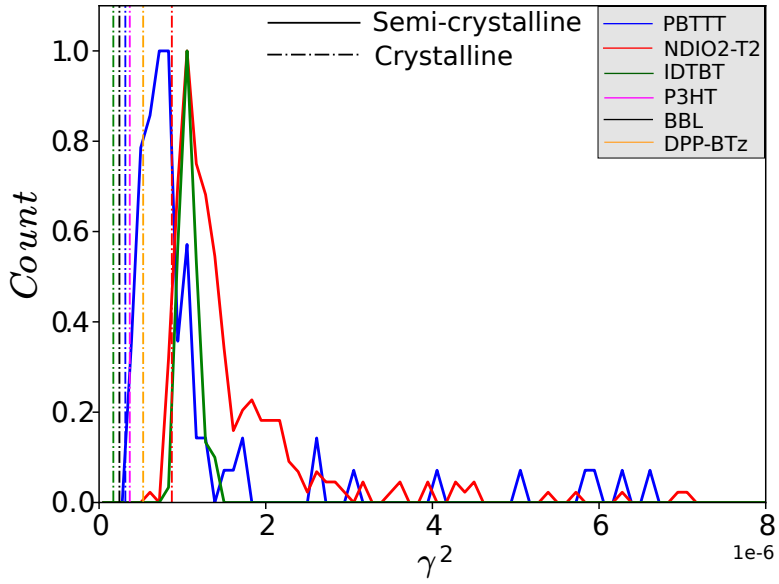

Figure 5.5: The distributions of γ^2 for polymer segments in a semi-crystalline morphology compared to corresponding crystalline geometries.

We report that a more localized charge leads to a larger spin-admixture. The same effect is also observed in chalcogenide molecules discussed in the section 5.1 where increasing the size of conjugated segment, for instance, in BXBX, DNXX and DAXX (X = Chalcogen) results in a corresponding decrease in γ. This effect has also been reported in Ref. [31]. This implies dependence of crystallite size on spin-relaxation rates in the polymer. A well ordered morphology, with a larger crystallite size, might have the charge delocalized to a larger unit which might lead to a smaller spin-mixing. However, the average charge-transfer rates might also be higher in such a morphology. Therefore, modeling spin-transport requires an intricate balance to be maintained between these two parameters to obtain required properties.

Therefore, for ordered polymers prepared using annealing, which gives rise to larger crystallite sizes, the spin-mixing would be smaller compared to disordered structures due to a large torsional degree of freedom between conjugated units, like P3HT. Moderation of the alkyl chains to reduce interdigitation or bulky groups adjacent to each other can lead to steric-hindrance which also distort the backbone polymer chain, leading to a larger spin-mixing. This behavior of spin-admixture can be used to tune spin-transport

no. monomers	IDTBT
1	$3.60 \cdot 10^{-7}$
2	$1.71 \cdot 10^{-7}$
3	$1.51 \cdot 10^{-7}$
4	$1.37 \cdot 10^{-7}$

Table 5.3: Variation in γ^2 w.r.t. number of monomers of IDTBT

via molecular design in these materials.

5.3 Spin-transport in high-mobility polymers

Preceding discussions have emphasized the significance and applications of an accurately calculated γ to give in-depth insights into the spin-relaxation in a wide range of molecules. This section takes it a step further to demonstrate it's predictive capabilities, particularly by benchmarking it against experiments[2] on highly interesting systems i.e. the high-mobility polymer systems. Recent experiments [21] investigate spin-transport in polymers PBTTT and P3HT using a non-local spin-valve device as shown in Fig. 5.6. The spins were pumped from the permalloy into the organic layer using ferromagnetic resonance. The spins are then carried along the organic layer to the other end of the device and the spin-current is detected in the platinum layer using inverse spin-Hall effect. Through these experiments, the spin-diffusion length is extracted in these polymers by varying the distance between the platinum and the permalloy.

These measurements reveal remarkably high spin-diffusion lengths for the polymers i.e. 600 nm for P3HT and 1200 nm for PBTTT. While this can be attributed to a small SOC in these molecules, this solely doesn't explain why the diffusion lengths are long compared to Ref. [102] and secondly, despite of having similar constituent elements, the two polymers have vastly different spin-diffusion lengths.

Given that the carrier concentrations in the polymers are extremely high ($\sim 10^{20} cm^{-3}$), contributions from exchange-interactions in spin-transport are

[2]The experiments discussed in the following text have been performed at Cavendish Laboratory (Cambridge University) in the group of Prof. Henning Sirringhaus.

expected to play a crucial role, therefore, to understand this in detail, we use the analytical model described in Ref. [27]. The original model assumes an exchange and hopping driven transport over a uniform distribution of hopping sites which was modified suitable to take into account the morphological and a quasi-1D transport owing to a semi-crystalline nature of morphology in these polymers. Furthermore, all the parameters used in the model are calculated entirely from first-principles. This has been described in detail in Appendix B.

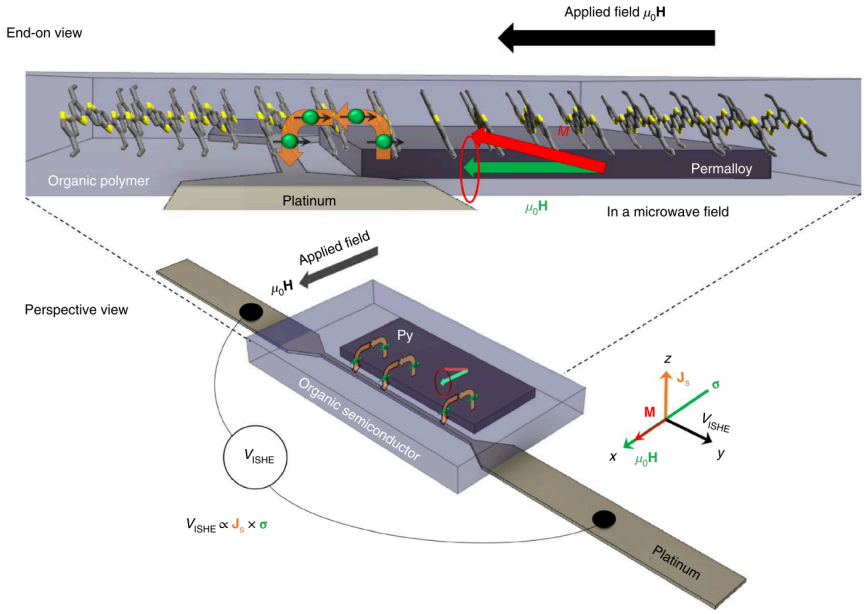

Figure 5.6: Schematic of a non-local spin-injection device used in Ref. [21]

As can be noted from the model, the spin-diffusion length (L_s) has a direct dependence on the exchange diffusion constant and the spin-relaxation is governed by the spin-admixture parameter. Hence, higher carrier-concentrations in addition to a smaller γ^2 for both the polymers would cause the L_s to be large. To explain differences between the two polymers, we use the same reasoning as in Section 5.2. P3HT has a large variation in dihedral angles (30-

60°) between thiophene units while PBTTT has virtually flat backbone. This is directly reflected in our γ^2 calculations where P3HT has $\gamma^2 = 2.42\times10^{-6}$, which is about an order of magnitude larger spin-mixing compared to PBTTT with a $\gamma^2 = 3.17\times10^{-7}$. Consequentially, the L_s is larger for the latter. Using the improved model, the dependence of L_s w.r.t. carrier concentrations can be calculated, these are presented in Fig. 5.7 compared against experimental data. The figure also compares our first-principle formulation with Yu's [39] method to calculate γ in order to highlight the accuracy and predictibility of this formulation.

Given the simplicity and approximation used in the model, our results show remarkable agreement with the experiments. However, it does not capture the dynamical effects present at the microscopic scale which are better described using a multiscale models.

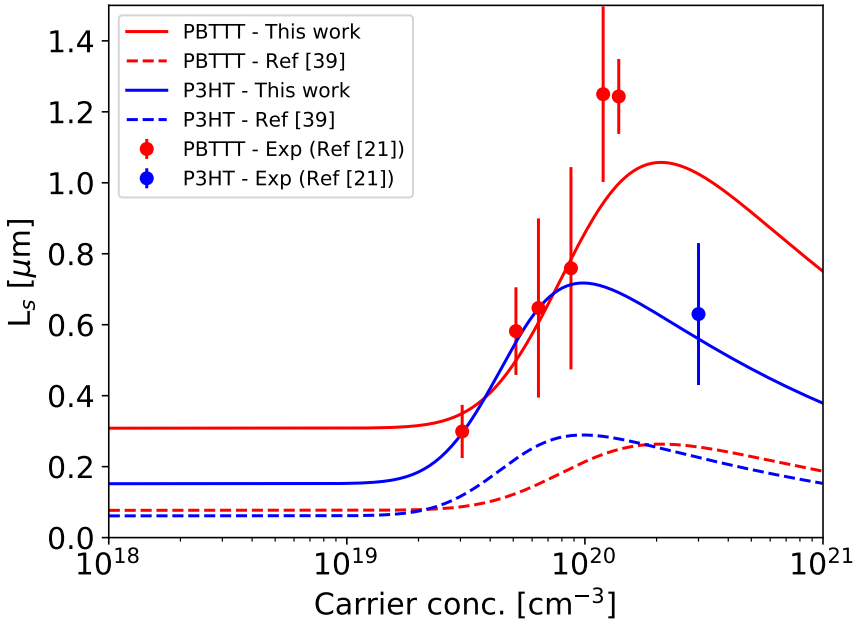

Figure 5.7: Spin-diffusion length in polymers. Experimental (dots) and calculated (lines) spin-diffusion lengths Ł$_s$ for PBTTT and P3HT as a function of carrier concentreation analytical curves calculated using γ from first-principles formalism (solid) vs approach used in Ref. [39]

5.4 Summary

Through the preceding discussion it became evident that not only γ is an extremely essential parameter in understanding spin-relaxation in organic semiconductors but also how the improved generalized mechanism to calculate γ is crucial to organic semiconductors. The method is transferable across systems, computationally inexpensive and has predictive capablities necessary for experiments.

It was found that γ doesn't necessarily follows the notion of SOC being proportional to Z^4 as it is defined for a particular spin-carrying molecular orbital which may or may not have contributions from atomic orbitals of a heavy element. This was studied in conjunction with elemental substitution. For the case of chalcogenide polymers, replacement with a heavier element led to an increase in γ however for metal-centered molecules like Alq_3 and phthalocyanine complexes (MPcs), the effect of substitution on γ did not correspond with atomic SOC strengths.

From the discussion it also became clear that this generalized formalism to calculate γ is transferable across different organic compounds, demonstrates the potential to be used for a high-throughput study and is extremely accurate.

In addition to it γ is a tremendous aid to understand spin-relaxation phenomenon occurring in most organic semiconductors. Strong correlation between T_1 of MPcs with γ suggested SOC as a driving factor of spin-relaxation. Furthermore, geometrical modifications in structure of molecules are precisely reflected in γ as was discussed using the example of high-mobility polymer systems. This also allowed for accurate predictions of spin-diffusion lengths in these systems.

The discussion also suggests that γ can be used as a design tool for tuning molecular SOC by chemical substitution or molecular geometry to achieve desirable effects in experiments.

Chapter 6

Final remarks and outlook

Organic semiconductors are potentially significant candidates for spintronic technology. First-principles theory can crucially aid our understanding of spin-dynamics in these materials ranging from single-molecule to material scales given a simulation technique of sufficient accuracy and transferability and low computational cost can be developed.

As pointed out in chapter 2, spin-relaxation pathways in organic semiconductors can be divided into five distinct mechanisms, namely the exchange and dipole interactions, Dyakonov-Perel like hyperfine relaxation, Elliot-Yafet like spin-flip hopping and the spin-phonon couplings. Out of these, the first three are well studied and several methodologies exist to parameterize them into first-principle models, but the Elliot-Yafet hopping and the spin-phonon coupling mechanisms offer much room for improvements.

The central theme of this thesis was modeling and tuning of spin-admixture in organic semiconductors to better understand the EY mechanism which is expected to be more important for high-mobility materials that form an important class of organic spintronics. At the core of both E-Y mechanism and the spin-phonon couplings lies the molecular spin-orbit coupling (SOC) that needs to be well defined.

6.1 Enhancing the SOC approximation

This essence of this work was generalization of the procedure to calculate spin-admixture parameter using an unrestricted Kohn-Sham formalism and the Zeroth Order Regular Approximation (ZORA) for the SOC operator as

opposed to using semi-empirical atomic SOC constants. ZORA is a two-component approximation to the Dirac equation and is variationally stable and non-perturbative. It is has been proven to be reliable for the weak SOC molecules discussed in the text.

However, one of the drawbacks of ZORA is that it is not gauge-invariant as the DFT ZORA energy depends on an effective potential. Therefore, large errors can be induced in case of calculations of binding energies. In addition to it, only one-body terms in the spin-orbit interaction are considered neglecting the many-body spin-same orbit and spin-other orbit interactions. While two-component methods such as ZORA are computationally inexpensive and work well to describe the relativistic effects in lighter molecules, in systems with much larger SOC and especially those with strong electronic correlations such as the f-shell molecules, ZORA might lead to inaccuracies. Hence, it is worthwhile looking into further approximations of the SOC operator.

One step to improve is to consider other effective potential methods within the realm of computationally inexpensive two-component methods such as the Douglas-Kroll-Hell approximation[82, 83] or a more accurate infinite order two-component methods (IOTC)[109]. Another ideal improvement is to reduce the four-component SOC Hamiltonian in form of an effective mean-field operator as discussed by Neese.[110] Here, the mean field SOC operator includes an approximation to the two-electron spin other orbit interactions in form of an effective single-electron operator therefore it is feasible to compute at a DFT level of theory.

Although computationally challenging, the four-component methods are even more accurate for elements with larger SOC however they require to go to computational techniques beyond DFT.

6.2 Spin-phonon coupling and multiscale spin-transport in organics

It was briefly discussed in chapter 2 that in addition to a hopping spin-flip mechanism, the SOC can also cause a local spin-relaxation driven by molecular vibrations. Such spin-flip transition can occur by either a direct Orbach transition [35] involving absorption or emission of single phonon or Raman-like processes [111] involving multiple phonons depending on the magnitude

of the external field applied. A schematic is shown in Fig. 6.1 below.

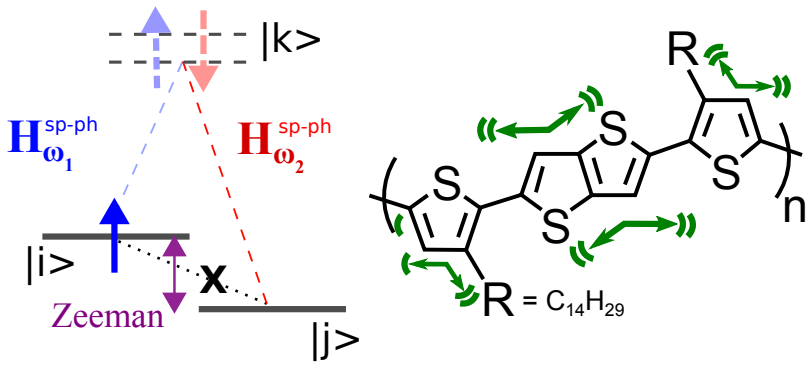

Figure 6.1: Intra-molecular spin-relaxation

At reasonable experimental magnetic fields $\sim$ 1 T, the corresponding Zeeman energy ($\sim$1 meV) is usually at least an order of magnitude smaller than the lowest energy vibrational modes ($\sim$10 meV). This renders direct processes to be unlikely, therefore the spin-flip rates might be dominated by a second-order Raman process. Here, the SO interaction is coupled with the lattice vibrations, also known as the spin-phonon couplings. The transition is mediated via a virtual state with a corresponding absorption and emission of two phonons whose energies are resonant with the Zeeman energy. Presence of Raman like processes are also hinted in recent works of Lunghi *et al.*[44, 46]

In a future work, we're trying to model these second-order Raman transitions using the Fermi's golden rule. This would allow us to calculate transition rates of such events originating from spin-phonon couplings and analyze the contributions from different phonon modes to the spin-relaxation. In addition to the SOC, HF interactions are also known to contribute to the spin-phonon couplings as noted in the works of Erlingsson *et al.*[112, 113] and can be treated similarly as SOC in our model. This would further enable us to calculate the parameters from all spin-relaxation mechanisms discussed in chapter 2.

A successful technique for calculating the spin-phonon couplings would accomplish a first-principle description of all the relevant spin-relaxation mechanisms from first-principles. An accurate description of these mechanisms at the molecular scale forms the basis for modeling more complex transport at the device scale. This can be further integrated all together into

an all-round multi-scale framework for spin-transport in organics equivalent to VOTCA-CTP[114] where the spin-dynamics and charge-dynamics are simultaneously evaluated for a realistic organic morhphology. This would be revolutionary approach in the field of organic spintronics as such a framework would facilitate a full-fledged investigation of spin-relaxation within organic semiconductors with explicit coupling to the charge dynamics.

It is evident that much remains to be explored in the field of organic spintronics that invites contribution from all spheres. The essence of this theoretical work lies in achieving a complementarity with disciplines of materials science and electronics with the end goal to manufacture an actual working device.

Appendix A

Comparison with g-tensor shift

A.1 Comparison with Δg

Deviation from the free-electron gyromagnetic factor is a widely used method to estimate the strength of spin-orbit coupling (SOC). This can be directly measured using the electron paramagnetic resonance (EPR) techniques.

The relation between the spin-admixture parameter, γ and Δg was initially explored in Ref. [39] and it was determined that the two measures of SOC are directly proportional to each other and scale with atomic spin-orbit coupling constants.

To investigate this relationship, we compare the values of γ calculated for molecules in the main text against the Δg values calculated in Ref. [104] and find how the two quantities correlate with each other.

From the Fig. A.1 it is apparent that when all the molecules are considered, the two values correlate with an r^2 value of 0.562. However, on excluding a certain outliers, the correlation increases with an r^2 of 0.935. This effect can be understood on comparing the expressions for the two quantities. It has been previously explored that main contribution to g-tensors for organic molecules is due to the orbital-Zeeman and SOC terms which can be expressed as follows,

$$g_{\mu\nu}^{(\mathrm{OZ/SOC})} = \sum_{k,l} \frac{\partial P_{kl}^{\alpha-\beta}}{\partial B_\mu} \langle \phi_k | \, h_\nu^{\mathrm{SOC}} \, | \phi_l \rangle \tag{A.1}$$

The first term represents the magnetic response to a local HF field (B_μ) on the spin-density ($P_{\alpha-\beta}$) and the second term includes SOC matrix elements,

similar γ, as used in 4.5. Therefore, the two terms differ only by a response term.

We note here that the outliers in Fig. A.1 correspond to the C-type isomers of BXBX class of molecules which have a different spin-density profiles.

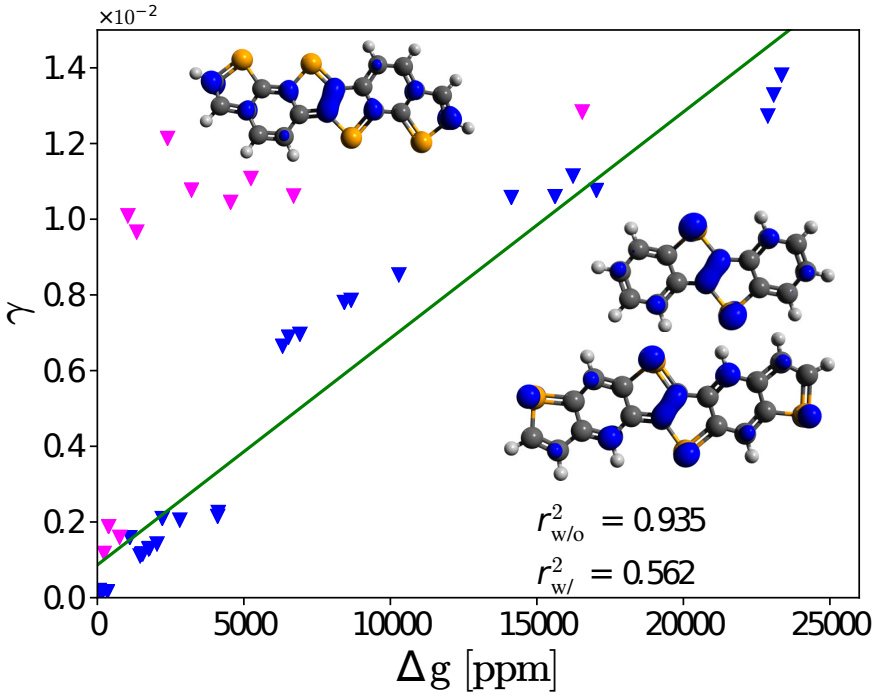

Figure A.1: Correlation between Δg and γ

We find that the absence of spin density from the chalcogenide atoms implies a negligible response term and therefore leads to a small Δg; however, since γ is independent of the response, it remains unaffected with variation in spin density.

While g-factor shifts can be used to characterize the SOC in organic compounds, it is important to note that γ represents the extent of mixing in a particular molecular orbital due to SOC.

Appendix B

Exchange enhanced transport in polymers

To model spin-diffusion length we use the model described in Ref. [47] and adopt it according to the quasi one-dimentional transport. The spin-diffusion lenght is defined as

$$\lambda = \sqrt{DT_1} \tag{B.1}$$

where D is the total diffusion constant with contributions from the exchange the hopping transport i.e. $D = D_{hop} + D_{ex}$ and the spin-relaxation time, $T_1 = (\omega_{SOC} + \omega_{HFI})^{-1}$ is due to the spin-orbit coupling (SOC) and hyperfine interaction (HFI).

The hopping diffusion constant, $D_{hop} = \mu k_B T/e$ where the mobilities (μ) for PBTTT and P3HT at 300 K are 1 $cm^2V^{-1}s^{-1}$ and 0.1 $cm^2V^{-1}s^{-1}$ respectively.

The exchange spin-diffusion constant, $D_{ex} = 1.6\ J(R)\ R^2$, where the J(R) describes the distance dependence of exchange interaction and R is the average distance between polarons which can be expressed as $J(R) = 0.821\ (e/\epsilon\xi)\ (R/\xi)^{5/2}\ e^{-2R/\xi}$ where e is the fundamental electronic charge and $\epsilon = 2$ is the dielectric constant that assumes a typical value for organic compounds. ξ defines the extent of delocalization of the polaron that is estimated from first-principle calculations.

To determine ξ three segments of PBTTT in a $\pi-\pi$ stacking arrangement are considered with a separation of 3.8 $\mathring{A}$ [115]. Using constrained-DFT, a charge on the middle segment is localized. The average spin-density is then

plotted along the y-direction in the Fig. B.1.

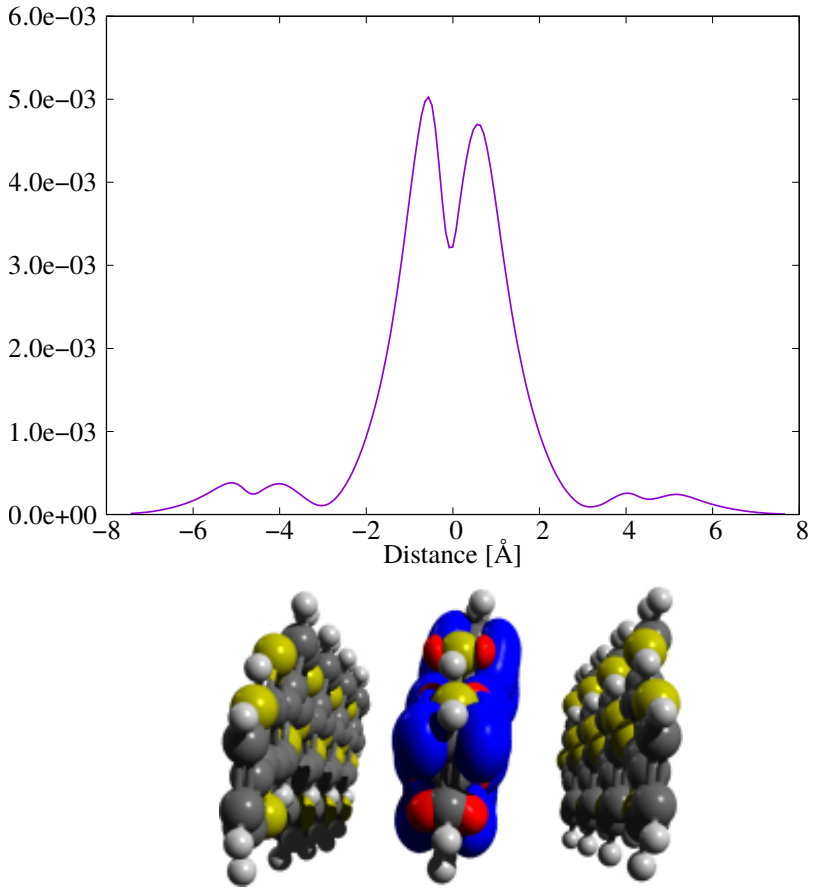

Figure B.1: Spin-density profile along $\pi-$stacking direction for PBTTT morphology.

From the figure, it is apparent that the polaron extent (ξ) on the middle backbone (centered at 0) is about $4\mathring{A}$ the direction of transport.

The spin-relaxation due to HFI, $\omega_{HFI} = 2\,\Omega_{HFI}^2\tau/3$, where $\Omega_{HFI} = 2\times10^8$ Hz corresponding to a HFI field of 10 G. The dwell time, $\tau = 2D_{hop}/a^2 + 2D_{ex}/R^2)^{-1}$ is a measure of the time interval between consecutive hops and a = 4 $\mathring{A}$, the average hopping distance between polarons in $\pi - \pi$ stacking direction.

The spin-relaxation rate due to the SOC is $\omega_{SOC} = 2\chi^2\tau^{-1}$, where $\chi^2 = (4/3)\gamma^2$ is the spin-mixing parameter due to the SOC. The calculated γ^2 for

PBTTT and P3HT are 3.15 $\times 10^{-7}$ and 2.42 $\times 10^{-6}$ respectively.

List of Publications

[1] U. Chopra, S. Shambhawi, S. A. Egorov, J. Sinova, and E. R. McNellis, "Accurate and general formalism for spin-mixing parameter calculations," *Phys. Rev. B*, vol. 100, p. 134410, oct 2019.

[2] U. Chopra, S. A. Egorov, J. Sinova, and E. R. McNellis, "Chemical and Structural Trends in the Spin-Admixture Parameter of Organic Semiconductor Molecules," *J. Phys. Chem. C*, vol. 123, pp. 19112–19118, aug 2019.

[3] S.-J. Wang, D. Venkateshvaran, M. R. Mahani, U. Chopra, E. R. McNellis, R. Di Pietro, S. Schott, A. Wittmann, G. Schweicher, M. Cubukcu, K. Kang, R. Carey, T. J. Wagner, J. N. M. Siebrecht, D. P. G. H. Wong, I. E. Jacobs, R. O. Aboljadayel, A. Ionescu, S. A. Egorov, S. Mueller, O. Zadvorna, P. Skalski, C. Jellett, M. Little, A. Marks, I. McCulloch, J. Wunderlich, J. Sinova, and H. Sirringhaus, "Long spin diffusion lengths in doped conjugated polymers due to enhanced exchange coupling," *Nat. Electron.*, vol. 2, pp. 98–107, mar 2019.

[4] S. Schott, U. Chopra, V. Lemaur, A. Melnyk, Y. Olivier, R. Di Pietro, I. Romanov, R. L. Carey, X. Jiao, C. Jellett, M. Little, A. Marks, C. R. McNeill, I. McCulloch, E. R. McNellis, D. Andrienko, D. Beljonne, J. Sinova, and H. Sirringhaus, "Polaron spin dynamics in high-mobility polymeric semiconductors," *Nat. Phys.*, vol. 15, pp. 814–822, aug 2019.

Bibliography

[1]G. E. Moore, "Cramming more components onto integrated circuits, Reprinted from Electronics, volume 38, number 8, April 19, 1965, pp.114 ff.", IEEE Solid-State Circuits Soc. Newsl. **11**, 33–35 (2006).

[2]Wikipedia contributors, *List of intel cpu microarchitectures — Wikipedia, the free encyclopedia*, (2020) `https://en.wikipedia.org/w/index.php?title=List_of_Intel_CPU_microarchitectures&oldid=943166098`.

[3]V. A. Dediu, L. E. Hueso, I. Bergenti, and C. Taliani, "Spin routes in organic semiconductors", Nat. Mater. **8**, 707–716 (2009).

[4]N. F. Mott, "The Electrical Conductivity of Transition Metals", Proc. R. Soc. A Math. Phys. Eng. Sci. **153**, 699–717 (1936).

[5]G. Binasch, P. Grünberg, F. Saurenbach, and W. Zinn, "Enhanced magnetoresistance in layered magnetic structures with antiferromagnetic interlayer exchange", Phys. Rev. B **39**, 4828–4830 (1989).

[6]M. N. Baibich, J. M. Broto, A. Fert, F. N. Van Dau, F. Petroff, P. Eitenne, G. Creuzet, A. Friederich, and J. Chazelas, "Giant magnetoresistance of (001)Fe/(001)Cr magnetic superlattices", Phys. Rev. Lett. **61**, 2472–2475 (1988).

[7]M. Julliere, "Tunneling between ferromagnetic films", Phys. Lett. A **54**, 225–226 (1975).

[8]T. Miyazaki and N. Tezuka, "Giant magnetic tunneling effect in Fe/Al2O3/Fe junction", J. Magn. Magn. Mater. **139**, L231–L234 (1995).

[9]J. M. Daughton, "Magnetoresistive memory technology", Thin Solid Films **216**, 162–168 (1992).

[10]Z. V. Vardeny, S. Majumdar, H. Majumdar, R. Österbacka, and Z. V. Vardeny, *Organic Spintronics*, edited by Z. Vardeny, Vol. 1-5 (CRC Press, Apr. 2010), pp. 1–335.

[11]S. Sanvito, "Molecular spintronics", Chem. Soc. Rev. **40**, 3336 (2011).

[12]A. Cornia and P. Seneor, "Spintronics: The molecular way", Nat. Mater. **16**, 505–506 (2017).

[13]A. Hagfeldt, G. Boschloo, L. Sun, L. Kloo, and H. Pettersson, "Dye-Sensitized Solar Cells", Chem. Rev. **110**, 6595–6663 (2010).

[14]O. Inganäs, "Organic Photovoltaics over Three Decades", Adv. Mater. **30**, 1800388 (2018).

[15]C. Wang, H. Dong, W. Hu, Y. Liu, and D. Zhu, "Semiconducting π-Conjugated Systems in Field-Effect Transistors: A Material Odyssey of Organic Electronics", Chem. Rev. **112**, 2208–2267 (2012).

[16]L. Torsi, M. Magliulo, K. Manoli, and G. Palazzo, "Organic field-effect transistor sensors: a tutorial review", Chem. Soc. Rev **42**, 8612 (2013).

[17]R.-P. Xu, Y.-Q. Li, and J.-X. Tang, "Recent advances in flexible organic light-emitting diodes", J. Mater. Chem. C **4**, 9116–9142 (2016).

[18]V. Dediu, M. Murgia, F. Matacotta, C. Taliani, and S. Barbanera, "Room temperature spin polarized injection in organic semiconductor", Solid State Commun. **122**, 181–184 (2002).

[19]Z. H. Xiong, D. Wu, Z. V. Vardeny, and J. Shi, "Giant magnetoresistance in organic spin-valves", Nature **427**, 821–824 (2004).

[20]J. Tsurumi, H. Matsui, T. Kubo, R. Häusermann, C. Mitsui, T. Okamoto, S. Watanabe, and J. Takeya, "Coexistence of ultra-long spin relaxation time and coherent charge transport in organic single-crystal semiconductors", Nat. Phys. **13**, 994–998 (2017).

[21]S.-J. Wang, D. Venkateshvaran, M. R. Mahani, U. Chopra, E. R. McNellis, R. Di Pietro, S. Schott, A. Wittmann, G. Schweicher, M. Cubukcu, K. Kang, R. Carey, T. J. Wagner, J. N. M. Siebrecht, D. P. G. H. Wong, I. E. Jacobs, R. O. Aboljadayel, A. Ionescu, S. A. Egorov, S. Mueller, O. Zadvorna, P. Skalski, C. Jellett, M. Little, A. Marks, I. McCulloch, J. Wunderlich, J. Sinova, and H. Sirringhaus, "Long spin diffusion lengths in doped conjugated polymers due to enhanced exchange coupling", Nat. Electron. **2**, 98–107 (2019).

[22]P. A. M. Dirac, "The Quantum Theory of the Electron", Proc. R. Soc. A Math. Phys. Eng. Sci. **117**, 610–624 (1928).

[23]M. Dyakonov, V. Marushchak, V. I. Perel, and A. Titkov, "The effect of strain on the spin relaxation of conduction electrons in III-V semiconductors", Zh. Eksp. Teor. Fiz **90**, 1123 (1986).

[24]R. J. Elliott, "Theory of the Effect of Spin-Orbit Coupling on Magnetic Resonance in Some Semiconductors", Phys. Rev. **96**, 266–279 (1954).

[25]Y. Yafet, "g Factors and Spin-Lattice Relaxation of Conduction Electrons", in *Solid state phys. - adv. res. appl.* Vol. 14, edited by F. Seitz and D. Turnbull, C (Academic, New York, May 1963), pp. 1–98.

[26]V. Coropceanu, J. Cornil, D. A. da Silva Filho, Y. Olivier, R. Silbey, and J. L. Brédas, "Charge transport in organic semiconductors", Chem. Rev. **107**, 926–952 (2007).

[27]Z. G. Yu, F. Ding, and H. Wang, "Hyperfine interaction and its effects on spin dynamics in organic solids", Phys. Rev. B **87**, 205446 (2013).

[28]T. D. Nguyen, G. Hukic-Markosian, F. Wang, L. Wojcik, X.-G. Li, E. Ehrenfreund, and Z. V. Vardeny, "Isotope effect in spin response of π-conjugated polymer films and devices", Nat. Mater. **9**, 345–352 (2010).

[29]P. A. Bobbert, W. Wagemans, F. W. A. van Oost, B. Koopmans, and M. Wohlgenannt, "Theory for Spin Diffusion in Disordered Organic Semiconductors", Phys. Rev. Lett. **102**, 156604 (2009).

[30]Z. G. Yu, "Microscopic theory of electron spin relaxation in N@ C60", Phys. Rev. B **77**, 205439 (2008).

[31]J. Rybicki and M. Wohlgenannt, "Spin-orbit coupling in singly charged π-conjugated polymers", Phys. Rev. B **79**, 153202 (2009).

[32]J. Rybicki, T. Nguyen, Y. Sheng, and M. Wohlgenannt, "Spin–orbit coupling and spin relaxation rate in singly charged -conjugated polymer chains", Synth. Met. **160**, 280–284 (2010).

[33]A. Norambuena, E. Muñoz, H. T. Dinani, A. Jarmola, P. Maletinsky, D. Budker, and J. R. Maze, "Spin-lattice relaxation of individual solid-state spins", Phys. Rev. B **97**, 094304 (2018).

[34]L. Nuccio, M. Willis, L. Schulz, S. Fratini, F. Messina, M. D'Amico, F. L. Pratt, J. S. Lord, I. McKenzie, M. Loth, B. Purushothaman, J. Anthony, M. Heeney, R. M. Wilson, I. Hernández, M. Cannas, K. Sedlak, T. Kreouzis, W. P. Gillin, C. Bernhard, and A. J. Drew, "Importance of Spin-Orbit Interaction for the Electron Spin Relaxation in Organic Semiconductors", Phys. Rev. Lett. **110**, 216602 (2013).

[35]R. Orbach, "Spin-lattice relaxation in rare-earth salts", Proc. R. Soc. London. Ser. A. Math. Phys. Sci. **264**, 458–484 (1961).

[36]K. N. Shrivastava, "Theory of Spin–Lattice Relaxation", Phys. status solidi **117**, 437–458 (1983).

[37]C. A. Masmanidis, H. H. Jaffe, and R. L. Ellis, "Spin-orbit coupling in organic molecules.", J. Phys. Chem. **79**, 2052–2061 (1975).

[38]Z. G. Yu, "Spin-orbit coupling, spin relaxation, and spin diffusion in organic solids", Phys. Rev. Lett. **106**, 106602 (2011).

[39]Z. G. Yu, "Spin-orbit coupling and its effects in organic solids", Phys. Rev. B **85**, 115201 (2012).

[40]S. W. Jiang, S. Liu, P. Wang, Z. Z. Luan, X. D. Tao, H. F. Ding, and D. Wu, "Exchange-Dominated Pure Spin Current Transport in Alq_3 Molecules", Phys. Rev. Lett. **115**, 086601 (2015).

[41]A. J. Drew, J. Hoppler, L. Schulz, F. L. Pratt, P. Desai, P. Shakya, T. Kreouzis, W. P. Gillin, A. Suter, N. a. Morley, V. K. Malik, A. Dubroka, K. W. Kim, H. Bouyanfif, F. Bourqui, C. Bernhard, R. Scheuermann, G. J. Nieuwenhuys, T. Prokscha, and E. Morenzoni, "Direct measurement of the electronic spin diffusion length in a fully functional organic spin valve by low-energy muon spin rotation", Nat. Mater. **8**, 109–114 (2009).

[42]N. J. Harmon and M. E. Flatté, "Distinguishing Spin Relaxation Mechanisms in Organic Semiconductors", Phys. Rev. Lett. **110**, 176602 (2013).

[43]N. J. Harmon and M. E. Flatté, "Spin relaxation in materials lacking coherent charge transport", Phys. Rev. B **90**, 115203 (2014).

[44]A. Lunghi, F. Totti, S. Sanvito, and R. Sessoli, "Intra-molecular origin of the spin-phonon coupling in slow-relaxing molecular magnets", Chem. Sci. **8**, 6051–6059 (2017).

[45]A. Lunghi, F. Totti, R. Sessoli, and S. Sanvito, "The role of anharmonic phonons in under-barrier spin relaxation of single molecule magnets", Nat. Commun. **8**, 1–7 (2017).

[46]A. Lunghi and S. Sanvito, "Spin-Phonon Relaxation in Molecular Qubits from First Principles Spin Dynamics", (2019).

[47]Z. G. Yu, "Spin transport and the Hanle effect in organic spintronics", Nanoelectron. Spintron. **1**, 1–18 (2015).

[48]M. Cox, E. H. M. van der Heijden, P. Janssen, and B. Koopmans, "Investigating the influence of traps on organic magnetoresistance by molecular doping", Phys. Rev. B **89**, 085201 (2014).

[49]M. Kimata, D. Nozaki, Y. Niimi, H. Tajima, and Y. C. Otani, "Spin relaxation mechanism in a highly doped organic polymer film", Phys. Rev. B **91**, 224422 (2015).

[50]X. Zhang, S. Mizukami, Q. Ma, T. Kubota, M. Oogane, H. Naganuma, Y. Ando, and T. Miyazaki, "Spin-dependent transport behavior in C60 and Alq3 based spin valves with a magnetite electrode (invited)", J. Appl. Phys. **115**, 172608 (2014).

[51]T. L. Keevers and D. R. McCamey, "Measuring spin relaxation with standard pulse sequences in the singlet-triplet basis", J. Magn. Reson. **257**, 70–78 (2015).

[52]J. Rawson, P. J. Angiolillo, P. R. Frail, I. Goodenough, and M. J. Therien, "Electron Spin Relaxation of Hole and Electron Polarons in π-Conjugated Porphyrin Arrays: Spintronic Implications", J. Phys. Chem. B **119**, 7681–7689 (2015).

[53]S. Liang, R. Geng, B. Yang, W. Zhao, R. Chandra Subedi, X. Li, X. Han, and T. D. Nguyen, "Curvature-enhanced Spin-orbit Coupling and Spinterface Effect in Fullerene-based Spin Valves", Sci. Rep. **6**, 19461 (2016).

[54]A. V. Shumilin and V. V. Kabanov, "Kinetic equations for hopping transport and spin relaxation in a random magnetic field", Phys. Rev. B **92**, 014206 (2015).

[55]A. Droghetti, I. Rungger, M. Cinchetti, and S. Sanvito, "Vibron-assisted spin relaxation at a metal/organic interface", Phys. Rev. B **91**, 224427 (2015).

[56]V. V. Mkhitaryan and V. V. Dobrovitski, "Quantum dynamics of nuclear spins and spin relaxation in organic semiconductors", Phys. Rev. B **95**, 214204 (2017).

[57]N. Lu, N. Gao, L. Li, and M. Liu, "Temperature, electric-field, and carrier-density dependence of hopping magnetoresistivity in disordered organic semiconductors", Phys. Rev. B **96**, 165205 (2017).

[58]F. Jensen, *Introduction to Computational Chemistry, 3rd Edition* (Wiley, 2017).

[59]N. S. O. Attila Szabo, *Modern Quantum Chemistry: Introduction to Advanced Electronic Structure Theory* (Dover Science Books, 1996).

[60]R. O. Jones, "Density functional theory: Its origins, rise to prominence, and future", Rev. Mod. Phys. **87**, 897–923 (2015).

[61]M. Born and R. Oppenheimer, "Zur Quantentheorie der Molekeln", Ann. Phys. **389**, 457–484 (1927).

[62]D. R. Hartree, "The Wave Mechanics of an Atom with a Non-Coulomb Central Field. Part I. Theory and Methods", Math. Proc. Cambridge Philos. Soc. **24**, 89–110 (1928).

[63]C. C. J. Roothaan, "Self-Consistent Field Theory for Open Shells of Electronic Systems", Rev. Mod. Phys. **32**, 179–185 (1960).

[64]J. A. Pople and R. K. Nesbet, "Self-Consistent Orbitals for Radicals", J. Chem. Phys. **22**, 571–572 (1954).

[65]A. A. Ovchinnikov and J. K. Labanowski, *Simple spin correction of unrestricted density-functional calculation*, tech. rep. 6 (1996), pp. 3946–3952.

[66]K. Yamaguchi, F. Jensen, A. Dorigo, and K. N. Houk, "A spin correction procedure for unrestricted Hartree-Fock and Møller-Plesset wavefunctions for singlet diradicals and polyradicals", Chem. Phys. Lett. **149**, 537–542 (1988).

[67]L. H. Thomas, "The calculation of atomic fields", Math. Proc. Cambridge Philos. Soc. **23**, 542–548 (1927).

[68]E. Fermi, "Eine statistische Methode zur Bestimmung einiger Eigenschaften des Atoms und ihre Anwendung auf die Theorie des periodischen Systems der Elemente", Zeitschrift für Phys. **48**, 73–79 (1928).

[69]W. Hohenberg, P.; Kohn, "Hohenberg, P.; Kohn, W.", Phys. Rev. **136**, B864–B871 (1964).

[70]W. Kohn and L. J. Sham, "Self-Consistent Equations Including Exchange and Correlation Effects", Phys. Rev. **140**, A1133–A1138 (1965).

[71]J. P. Perdew, K. Burke, and M. Ernzerhof, "Generalized gradient approximation made simple", Phys. Rev. Lett. **77**, 3865–3868 (1996).

[72]A. D. Becke, "Density-functional exchange-energy approximation with correct asymptotic behavior", Phys. Rev. A **38**, 3098–3100 (1988).

[73]C. Lee, W. Yang, and R. G. Parr, "Development of the Colle-Salvetti correlation-energy formula into a functional of the electron density", Phys. Rev. B **37**, 785–789 (1988).

[74]J. Tao, J. P. Perdew, V. N. Staroverov, and G. E. Scuseria, "Climbing the Density Functional Ladder: Nonempirical Meta–Generalized Gradient Approximation Designed for Molecules and Solids", Phys. Rev. Lett. **91**, 146401 (2003).

[75]C. Adamo and V. Barone, "Toward chemical accuracy in the computation of NMR shieldings: The PBE0 model", Chem. Phys. Lett. **298**, 113–119 (1998).

[76]A. D. Becke, "Density-functional thermochemistry. III. The role of exact exchange", J. Chem. Phys. **98**, 5648–5652 (1993).

[77]A. J. Cohen, P. Mori-Sánchez, and W. Yang, "Insights into current limitations of density functional theory", Science (80-.). **321**, 792–794 (2008).

[78]G. Breit, "The Effect of Retardation on the Interaction of Two Electrons", Phys. Rev. **34**, 553–573 (1929).

[79]E. van Lenthe, J. G. Snijders, and E. J. Baerends, "The zero-order regular approximation for relativistic effects: The effect of spin–orbit coupling in closed shell molecules", J. Chem. Phys. **105**, 6505–6516 (1996).

[80]W. Pauli, "Zur Quantenmechanik des magnetischen Elektrons", Zeitschrift für Phys. **43**, 601–623 (1927).

[81]F. Neese and E. I. Solomon, "Calculation of Zero-Field Splittings, g-Values, and the Relativistic Nephelauxetic Effect in Transition Metal Complexes. Application to High-Spin Ferric Complexes †", Inorg. Chem. **37**, 6568–6582 (1998).

[82]M. Douglas and N. M. Kroll, "Quantum electrodynamical corrections to the fine structure of helium", Ann. Phys. (N. Y). **82**, 89–155 (1974).

[83]B. A. Hess, "Applicability of the no-pair equation with free-particle projection operators to atomic and molecular structure calculations", Phys. Rev. A **32**, 756–763 (1985).

[84]M. Ernzerhof and G. E. Scuseria, "Assessment of the Perdew-Burke-Ernzerhof exchange-correlation functional", J. Chem. Phys. **110**, 5029–5036 (1999).

[85]D. J. D. Wilson, C. E. Mohn, and T. Helgaker, "The rotational g tensor as a benchmark for density-functional theory calculations of molecular magnetic properties", J. Chem. Theory Comput. **1**, 877–888 (2005).

[86]F. Neese, "Prediction of electron paramagnetic resonance g values using coupled perturbed Hartree–Fock and Kohn–Sham theory", J. Chem. Phys. **115**, 11080–11096 (2001).

[87]C. J. Cramer and D. G. Truhlar, "Density functional theory for transition metals and transition metal chemistry", Phys. Chem. Chem. Phys. **11**, 10757 (2009).

[88]J. P. Perdew and Y. Wang, "Accurate and simple analytic representation of the electron-gas correlation energy", Phys. Rev. B **45**, 13244–13249 (1992).

[89]L. Bogani and W. Wernsdorfer, "Molecular spintronics using single-molecule magnets", in *Nanosci. technol.* Edited by Peter Rodgers (Nature Publishing Group) (Co-Published with Macmillan Publishers Ltd, UK, Aug. 2009), pp. 194–201.

[90]D. N. Woodruff, R. E. P. Winpenny, and R. A. Layfield, "Lanthanide Single-Molecule Magnets", Chem. Rev. **113**, 5110–5148 (2013).

[91]J. Heyd, G. E. Scuseria, and M. Ernzerhof, "Hybrid functionals based on a screened Coulomb potential", J. Chem. Phys. **118**, 8207–8215 (2003).

[92]A. V. Krukau, O. A. Vydrov, A. F. Izmaylov, and G. E. Scuseria, "Influence of the exchange screening parameter on the performance of screened hybrid functionals", J. Chem. Phys. **125**, 224106 (2006).

[93]M. Valiev, E. J. Bylaska, N. Govind, K. Kowalski, T. P. Straatsma, H. J. Van Dam, D. Wang, J. Nieplocha, E. Apra, T. L. Windus, and W. A. De Jong, "NWChem: A comprehensive and scalable open-source solution for large scale molecular simulations", Comput. Phys. Commun. **181**, 1477–1489 (2010).

[94]D. A. Pantazis, X.-Y. Chen, C. R. Landis, and F. Neese, "All-Electron Scalar Relativistic Basis Sets for Third-Row Transition Metal Atoms", J. Chem. Theory Comput. **4**, 908–919 (2008).

[95]P. Graziosi, A. Riminucci, M. Prezioso, C. Newby, D. Brunel, I. Bergenti, D. Pullini, D. Busquets-Mataix, M. Ghidini, and V. A. Dediu, "Pentacene thin films on ferromagnetic oxide: Growth mechanism and spintronic devices", Appl. Phys. Lett. **105** (2014) 10.1063/1.4890328.

[96]T. D. Nguyen, F. Wang, X. G. Li, E. Ehrenfreund, and Z. V. Vardeny, "Spin diffusion in fullerene-based devices: Morphology effect", Phys. Rev. B **87**, 1–7 (2013).

[97]D. Venkateshvaran, M. Nikolka, A. Sadhanala, V. Lemaur, M. Zelazny, M. Kepa, M. Hurhangee, A. J. Kronemeijer, V. Pecunia, I. Nasrallah, I. Romanov, K. Broch, I. McCulloch, D. Emin, Y. Olivier, J. Cornil, D. Beljonne, and H. Sirringhaus, "Approaching disorder-free transport in high-mobility conjugated polymers", Nature **515**, 384–388 (2014).

[98]K. Kang, S. Watanabe, K. Broch, A. Sepe, A. Brown, I. Nasrallah, M. Nikolka, Z. Fei, M. Heeney, D. Matsumoto, K. Marumoto, H. Tanaka, S. I. Kuroda, and H. Sirringhaus, "2D coherent charge transport in highly ordered conducting polymers doped by solid state diffusion", Nat. Mater. **15**, 896–902 (2016).

[99]X. Zhang, H. Bronstein, A. J. Kronemeijer, J. Smith, Y. Kim, R. J. Kline, L. J. Richter, T. D. Anthopoulos, H. Sirringhaus, K. Song, M. Heeney, W. Zhang, I. McCulloch, and D. M. Delongchamp, "Molecular origin of high field-effect mobility in an indacenodithiophene- benzothiadiazole copolymer", Nature Communications **4**, 1–9 (2013).

[100]R. Matsidik, A. Luzio, Ö. Askin, D. Fazzi, A. Sepe, U. Steiner, H. Komber, M. Caironi, and M. Sommer, "Highly Planarized Naphthalene Diimide-Bifuran Copolymers with Unexpected Charge Transport Performance", Chem. Mater. **29**, 5473–5483 (2017).

[101]M. Gruber, S. H. Jung, S. Schott, D. Venkateshvaran, A. J. Kronemeijer, J. W. Andreasen, C. R. McNeill, W. W. Wong, M. Shahid, M. Heeney, J. K. Lee, and H. Sirringhaus, "Enabling high-mobility, ambipolar charge-transport in a DPP-benzotriazole copolymer by side-chain engineering", Chem. Sci. **6**, 6949–6960 (2015).

[102]S. Watanabe, K. Ando, K. Kang, S. Mooser, Y. Vaynzof, H. Kurebayashi, E. Saitoh, and H. Sirringhaus, "Polaron spin current transport in organic semiconductors", Nat. Phys. **10**, 308–313 (2014).

[103]K. Ando, S. Watanabe, S. Mooser, E. Saitoh, and H. Sirringhaus, "Solution-processed organic spin–charge converter", Nat. Mater. **12**, 622–627 (2013).

[104]S. Schott, E. R. McNellis, C. B. Nielsen, H.-Y. Y. Chen, S. Watanabe, H. Tanaka, I. McCulloch, K. Takimiya, J. Sinova, and H. Sirringhaus, "Tuning the effective spin-orbit coupling in molecular semiconductors", Nat. Commun. **8**, 15200 (2017).

[105]E. R. McNellis, S. Schott, H. Sirringhaus, and J. Sinova, "Molecular tuning of the magnetic response in organic semiconductors", Phys. Rev. Mater. **2**, 074405 (2018).

[106]V. N. Prigodin, J. D. Bergeson, D. M. Lincoln, and A. J. Epstein, "Anomalous room temperature magnetoresistance in organic semiconductors", Synth. Met. **156**, 757–761 (2006).

[107]B. B. Chen, Y. Zhou, S. Wang, Y. J. Shi, H. F. Ding, and D. Wu, "Giant magnetoresistance enhancement at room-temperature in organic spin valves based on La0.67Sr0.33MnO3electrodes", Appl. Phys. Lett. **103**, 072402 (2013).

[108]K. Bader, M. Winkler, and J. van Slageren, "Tuning of molecular qubits: very long coherence and spin–lattice relaxation times", Chem. Commun. **52**, 3623–3626 (2016).

[109]M. Barysz and A. J. Sadlej, "Infinite-order two-component theory for relativistic quantum chemistry", The Journal of Chemical Physics **116**, 2696–2704 (2002).

[110]F. Neese, "Efficient and accurate approximations to the molecular spin-orbit coupling operator and their use in molecular g-tensor calculations", J. Chem. Phys. **122**, 034107 (2005).

[111]J. V. Vleck, "Paramagnetic relaxation times for titanium and chrome alum", Phys. Rev. (1940).

[112]S. I. Erlingsson and Y. V. Nazarov, "Hyperfine-mediated transitions between a Zeeman split doublet in GaAs quantum dots: The role of the internal field", Phys. Rev. B **66**, 155327 (2002).

[113]S. I. Erlingsson, Y. V. Nazarov, and V. I. Fal'ko, "Nucleus-mediated spin-flip transitions in GaAs quantum dots", Phys. Rev. B **64**, 195306 (2001).

[114]V. Rühle, C. Junghans, A. Lukyanov, K. Kremer, and D. Andrienko, "Versatile object-oriented toolkit for coarse-graining applications", J. Chem. Theory Comput. **5**, 3211–3223 (2009).

[115]E. Cho, C. Risko, D. Kim, R. Gysel, N. Cates Miller, D. W. Breiby, M. D. McGehee, M. F. Toney, R. J. Kline, and J. L. Bredas, "Three-dimensional packing structure and electronic properties of biaxially oriented poly(2,5-bis(3-alkylthiophene-2-yl)thieno[3,2- b]thiophene) films", J. Am. Chem. Soc. **134**, 6177–6190 (2012).